CHARACTERIZATION OF PIN DIODES

A Thesis Submitted
in Partial Fulfilment of the Requirements
for the Degree of
MASTER OF TECHNOLOGY

By
AKHIL AGRAWAL

to the
DEPARTMENT OF ELECTRICAL ENGINEERING
INDIAN INSTITUTE OF TECHNOLOGY, KANPUR
DECEMBER, 1980

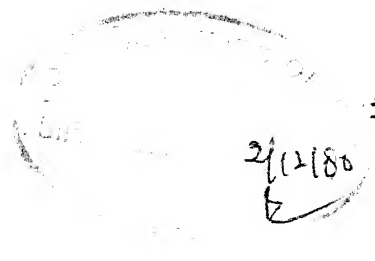

CERTIFICATE

This is to certify that the thesis entitled 'Characterization of PIN Diode' by Akhil Agrawal has been carried out under my supervision and has not been submitted elsewhere for a degree.

(M.M. Hasan)
Professor
Department of Electrical Engineering
Indian Institute of Technology
Kanpur.

December, 1980

ACKNOWLEDGEMENTS

I have a pleasure in expressing my deep sense of gratitude to Dr. M.M. Hasan for having suggested this problem to me. His constant guidance and encouragement throughout the work is beyond mention.

I thank Mr. A.K. Gupta for his valuable suggestions and help which he provided during the course of this thesis.

Thanks are also due to Rashmi, Anshoo, Neeru and Neelam didi for helping me in the preparation of the final phase of my thesis I should not forget to mention Usha didi and Girish who provided constant moral support during the moment of depression. I should also thank Lav and R.K. Pandey for providing help time to time.

A lot is left unsaid for my parents whose constant encouragement has made this work possible in the present state.

Finally I thank Mr. C.M. Abraham for his neat and efficient typing.

Akhil Agrawal

CONTENTS

ABSTRACT

The forward I-V characteristics and forward resistance of the PIN diodes are calculated with the band gap narrowing effect taken into consideration. It is found that at low currents, the band gap narrowing affects the forward resistance of PIN diode. At high currents, the BGN modifies the I-V characteristics. An optimum life time is also found at which the forward voltage is minimum.

In the reverse characteristics of PIN diode the breakdown voltage is studied. The dependence of breakdown voltage on impurity gradient is seen and it is noticed that the knowledge of impurity gradient is necessary for the accurate prediction of breakdown voltage.

CHAPTER 1

INTRODUCTION

Ever since the PIN diode was first discovered by W.B. Prince [1] as a high voltage rectifier with a low forward resistance, it is finding more and more applications. Ulhir [2] in 1950 has pointed out its microwave potential. Since then, it has been used invariably as a microwave semiconductor device. Besides being used as a high voltage rectifier at low frequencies, there are high frequency applications as microwave switch, attenuator, modulator, phase shifter and protector etc. PIN diode offers high response speed, compactness, long life and high reliability.

1.1 THE PIN DIODE PARAMETERS AND THEIR IMPORTANCE

The diode parameters which are important for the above mentioned applications are :

(a) Junction capacitance

(b) Switching time

(c) Forward resistance

(d) Breakdown voltage

PIN diode, while used as a microwave switch, can be series or shunt connected. While used as a shunt connected, the switch shall be 'off' when it is forward biased and 'on' when reverse biased. In series connection, the switch is 'on'

when the diode is forward biased and 'off' when reverse biased. The performance of the switch is measured in terms of isolation when it is 'off' and in terms of insertion loss when it is 'on'. Where isolation is defined as the ratio (in dbs) of power incident at input to the power transmitted by the switch when it is in 'off' condition and insertion loss is defined as the ratio (in dbs) of the power incident at the input to the power transmitted by the switch when it is in 'on' condition.

The junction capacitance is an important parameter from frequency point of view. It limits the highest frequency at which the PIN diode can be used. As the capacitance increases the reactance at a particular frequency decreases and hence the insertion loss increases while used as a shunt connected (and isolation decreases if used as a series connected).

The switching time of the diode gives the information about the speed of transition from forward biased state to the reverse biased state and vice-versa. The switching time depends upon the power which the diode is supposed to handle. The higher is the power handled, higher will be the switching time of the diode.

The forward resistance of the PIN diode, at a particular bias current fixes the isolation if it is used in a shunt connecti (and insertion loss if used in a series connection). Since in different applications it is biased at different current, it is

important to know the dependence of forward resistance on forward current accurately. It will be then quite useful for device designer in designing a suitable device with exact specifications. Hence there is a need to find out the accurate I-V characteristics so the forward resistance dependence on forward current could also be calculated.

The breakdown voltage determines the upper limit of d.c. voltage upto which a PIN diode can be used in reverse direction. Therefore, it determines the power handling capability which is also dependent on frequency.

1.2 THE DIODE CHARACTERISTICS

The forward resistance and the breakdown voltage depends on the following material parameters.

(a) base region width
(b) base region doping
(c) minority carrier life time
(d) diode geometry

1.2.1 The Forward I-V Characteristics

So far a lot of work has been done in order to investigate the forward I-V characteristics of diode and to find out the effect of base region doping, base region width and carrier life time on its behaviour. Though the PIN diode in the present form was first proposed by Prince [1] in 1956,

Hall [3] in 1952 gave a theory for similar type of structure. He assumed that the total forward current is due to the recombination in the middle region only. Kleinman [4] then proposed a theory in which he neglected recombination in the base and found $\exp(V/V_T)$ dependence of current at low currents and V^2 dependence at high current . Fletcher later found that the current varies as V^2 at higher currents but at lower current the dependence is of $\exp(V/2V_T)$ nature, which was found by Hall also. The conflicting theory of Kleinman is due to his inadequate treatment of carrier life time in the base region. Fletcher further found that changes in mobility and life time does not change the I-V characteristics appreciably. Howard and Johnson [6] suggested V^2 dependence at higher currents after including carrier - carrier scattering effect also. But this dependence is valid only when $W/L < 1$ (where W is the base region width and L is the diffusion length in the base) and carrier concentration in the base is less then $10^{16}/cm^3$. When $W/L > 1$ or carrier concentration increases more than $10^{16}/cm^3$, the current varies as V^n where n is greater than 1. Herlet and Spenke [7] analysed PIN diode I-V characteristics without taking injection efficiency to be unity i.e. they considered the end region currents also, and found that this effects the J-V characteristics considerably.

Choo [8] examined the influence of life-time on J-V characteristics and found that at optimum life time a minimum in forward voltage drop occurs for a certain value of current. The effect of base width and doping on J-V characteristics has been studied by Kao and Muss [9] as well as by Graham and Hauser [10] . Kao and Muss calculated a theoretical limit on forward voltage drop for a particular breakdown voltage. Graham and Hauser found $\exp(V/2V_T)$ relationship for low base doping which, for high base doping, changes from $\exp(V/2V_T)$ to $\exp(V/V_T)$ and further to $\exp(V/2V_T)$ as the voltage is increased.

As could be seen from the fore-mentioned analysis that the effect of band gap narrowing on PIN diode J-V characteristics , has not been included by any of the workers. It has been observed experimentally that the forward voltage drop across PIN diode is higher than that has been calculated theoretically. The inclusion of band gap narrowing has already explained the discrepency between the experimentally observed injection efficiency and the theoretical predicted one [11] . It has also explained the temperature dependence of transistor current gain [12] . The influence of band gap narrowing on minority carrier current was found by De Man [13] . With the help of this Van Overstraeten [14] later explained the discrepency of emitter efficiency at higher currents. Keeping this in mind, the effect of band gap narrowing on PIN diode forward characteristics has been studied in

the present work. It was found that though the band gap narrowing does not effect the J-V characteristics at low currents, it does affect the forward resistance. At higher currents, band gap narrowing modifies the J-V characteristics also.

1.2.2 The Reverse J-V Characteristics

In the reverse bias state, the breakdown voltage was calculated by Van Overstraeten [15] . He assumed constant doping in the P^+ and N^+ region and also solved a simplified ionization integral equation in the base region. Moreover, the effect of depletion region width in P^+ and N^+ region was not taken into consideration. It was found, however, that the theoretical breakdown voltage is much higher than the observed breakdown voltage. The reasons for the discrepency are the impurity gradients at the two junctions, surface characteristics such as surface state charges and the dielectric coating at the surface which alters the surface electric field.

An attempt, in the present work, has been made to study the effect of impurity gradient at the junctions, the impurity gradient being one of the many factors responsible for the lowering of breakdown voltage. One dimensional numerical analysis, with constant, exponential and Gaussian doping profile in the heavily doped regions has been done and breakdown voltage is calculated by solving exact ionization integral. It is found that impurity gradient at the junctions does affect the breakdown

voltage and an accurate knowledge of the diffused minority profile is necessary to predict correct breakdown voltage.

1.3 OVERVIEW

In Chapter 2, the forward J-V characteristics is discussed. Firstly, the previous theory of Hall is given. Then, the forward J-V characteristics is calculated with the reduction in band gap due to higher impurity/carrier concentration being considered.

The forward resistance of PIN diode has been calculated, in Chapter 3 using the forward J-V characteristics of last chapter. The affect of band gap narrowing, base width and life time on forward resistance is also discussed in this chapter.

Chapter 4 deals with the breakdown voltage of PIN diode. The breakdown voltage is calculated for different impurity profiles in heavily doped regions. Then, the factors causing the reduction in breakdown voltage are discussed. Finally, some geometries to improve breakdown voltage are described.

The conclusions of the present work constitutes the last chapter.

CHAPTER 2

EFFECT OF BAND GAP NARROWING ON FORWARD CHARACTERISTICS

The forward J-V characteristics of PIN diodes have been a subject of extensive studies. In the present chapter, the effect of band gap narrowing on the forward characteristics is found and discussed. The first section deals with the band gap narrowing effect, its origin and empirical relations given by various investigators. This is followed by the derivation of modified relationship between current density and voltage for low and high currents. In the last section the results are discussed.

2.1 BAND GAP NARROWING

The band gap narrowing occurs in heavily doped semiconductors. This can be explained in two ways. The first is the overlapping of wave function with the increase in impurity atom concentration. As the impurity atom concentration increases, the average distance between these atoms decreases. Therefore, the mutual interaction between the impurity atoms increases which results in the overlapping of wave function. The overlapping leads to the split of energy level of individual atoms into a band of energy known as impurity band. The other mechanism by which the band gap narrowing is explained is the random distribution of impurity atoms in the crystal. To explain, let an arbitrary impurity atom is isolated. Now the effect of all the

other impurity atoms on the potential energy of electron associated with the isolated impurity atom could be calculated. As different impurity atoms will be considered, the potential energy will be different. This is due to the fact that impurity atoms are randomly distributed. The difference in the potential energy will lead to the split of ionization energy of impurity atoms which is detected as broadening of impurity levels.

Obviously, the width of the impurity band will increase with the increase in the concentration of impurity atoms. At high concentrations, the upper edge of the impurity band merges in the conduction band for n type semiconductor (for p type semiconductor, the bottom edge of impurity band merges in the valance band), under these circumstances, one can not speak off impurity band and conduction band literally, as single continuous band emerges resulting in band gap narrowing. Recently, Lanyon and Tuft [16] explained that band gap narrowing occurs due to the screening of minority carrier charge by the majority carriers. Therefore, in the device where high level injection occurs. it is the charge carriers which cause band gap narrowing.

Different workers have given different empirical formula to determine band gap narrowing quantitatively. Volfson and Subashiev [17] in 1967 investigated experimentally the fundamental optical absorption edge of silicon and found changes in the bandgap only for impurity concentrations above $1.85 \times 10^{19}/cm^3$. They have found that

$$\Delta E_g = K_1 (N_D^{1/3} - N_d^{1/3}) \qquad (2.1)$$

where ΔE_g = band gap narrowing, eV

$K_1 = 3.4 \times 10^{-8}$

N_D = impurity atoms concentration/cm^3

$N_d = 1.85 \times 10^{19}/cm^3$.

Band gap narrowing in silicon has been determined in the base region of bipolar transistors by Slotboom [18] . This effect becomes important for impurity concentration greater than about $10^{17}/cm^3$. The experimentally derived band gap narrowing as a function of impurity concentration is given by the following empirical formula

$$\Delta E_g = V_1 \, (F + \sqrt{(F^2 + C)})$$

where $V_1 = 9$ meV

$F = \ln(N/N_o)$

N = impurity atom concentration

$N_o = 10^{17}/cm^3$

$C = 0.5$

Lanyon and Tuft [16] determined band gap narrowing theoretically and compared the results with the experimental results. They suggested

$\Delta E_g = 22.5(N/10^{18})^{\frac{1}{2}}$ meV 2.3(a) for $3 \times 10^{17} < n < 2 \times 10^{19}$

$\Delta E_g = 162 \, (N/10^{20})^{1/6}$ meV 2.3(b) for $5 \times 10^{19} < n < 1.5 \times 10^{20}$

where

N = impurity atom concentration, cm^{-3}

The band gap narrowing, given by the above relationships, is plotted in Fig. 2.1 as a function of impurity atom concentration. Only the last two relationships, i.e. eqn. (2.2) and eqn. (2.3) are used in the investigation of present chapter.

The consequences of the band gap narrowing is creation of an electric field in the heavily doped semiconductor and the modification in the intrinsic carrier concentration. The electric field is given by

$$E_o = \frac{1}{q} \frac{d}{dx} (\Delta E_g) \tag{2.4}$$

while the intrinsic carrier concentration, i.e., in the heavily doped semiconductor is given by

$$nie^2(x) = n_{io}^2 \exp\left(\frac{\Delta E_g}{kT}\right) \tag{2.5}$$

where n_{io} is the intrinsic carrier concentration in the light doped semiconductors.

2.2 CARRIER TRANSPORT IN PIN DIODE

The previous theory of Hall [3] is based on the following assumptions.

(a) Unit injection efficiency at both the junction, i.e. the forward current consists of the current due to recombination in

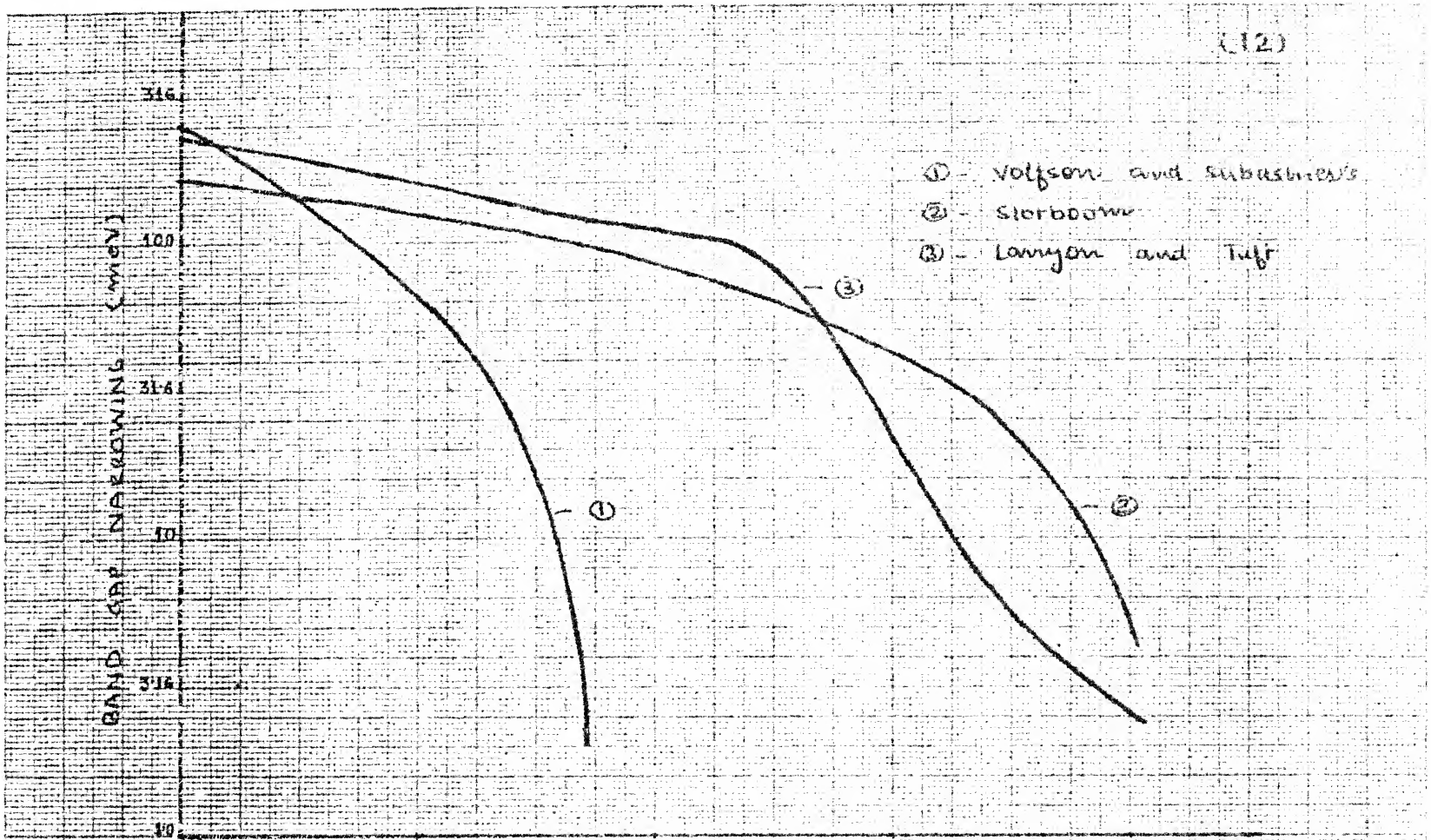

Fig (2.1) Band Gap Narrowing (BGN) using different empirical relations.

the middle region only, the end region currents being too small are neglected.

(b) The ambipolar diffusion length is constant over the entire middle region.

(c) The total voltage drop across the PIN diode is the sum of the voltage drops across junctions. The drop across middle region, being negligibly small, is neglected.

With these assumptions and starting with the continuity equation. Hall has derived the following equation between the current density J and the total voltage drop V.

$$J = \frac{2q D_a n_i}{W/2} F\left(\frac{W}{2L_a}\right) \cdot \exp\left(\frac{qV_a}{2kT}\right) \qquad (2.6a)$$

where

$$F\left(\frac{W}{2L_a}\right) = \left(\frac{W}{2L_a}\right) \tanh\left(\frac{W}{2L_a}\right) \left[1 - b^2 \tanh^4\left(\frac{W}{2L_a}\right)\right]^{-\frac{1}{2}} \qquad (2.6b)$$

The equation (2.6a) bears a striking similarity to that for high level injection in n^+P diode.

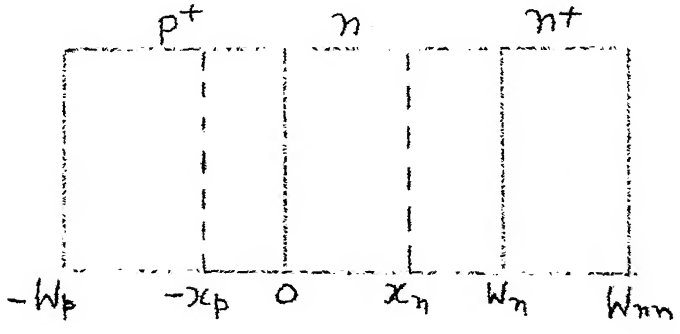

Fig. (2.2) The $P^+N\ N^+$ Diode

2.3 J-V CHARACTERISTICS OF PIN DIODE INCLUDING BGN EFFECT

2.3.1 At Low Currents

Let us consider a $P^+N\,N^+$ diode as shown in Fig. 2.2. Let E_o be the electric field produced by the band gap narrowing in the I region. Then the total electric field in the I region will be $(E+E_o)$. Now the two current equations and the continuity equation can be written as

$$J_p = q\,p\;\mu_p(E + E_o) - q\,Dp\,\frac{dp}{dx} \tag{2.7}$$

$$J_n = q\;\mu_n(E + E_o) + q\,Dn\,\frac{dn}{dx} \tag{2.8}$$

$$\frac{dJ_p}{dx} = -\frac{dJ_n}{dx} = -\frac{qp}{\tau} \tag{2.9}$$

The continuity equation (2.9) is written for high level injection and therefore the following relationship will hold good.

$$n(x) = p(x) \tag{2.10}$$

$$\frac{\partial n(x)}{\partial x} = \frac{\partial}{\partial x}\,p(x) \tag{2.11}$$

The electric field in the middle region can be written by combining eqn. (2.7) and (2.8) with (2.10) and (2.11).

$$J_n + J_p = q\,p(E + E_o)\,(\mu n + \mu p) + q\,\frac{dp}{dx}\,(D_n - D_p)$$

$$J = J_n + J_p = qp\,\mu p(1+b)(E+E_o) + qD_p(b-1)\,\frac{dp}{dx}$$

or

$$E+E_o = -\frac{J}{qp\mu_p(1+b)} - \frac{KT}{q}\,\frac{q\mu_p(b-1)}{q\mu_p p(b+1)} \cdot \frac{dp}{dx}$$

or

$$E = -\frac{J}{qp\mu_p(1+b)} - \frac{KT}{q}\,\frac{b-1}{b+1} \cdot \frac{1}{p}\,\frac{dp}{dx} - E_o$$

or

$$E = -\frac{J}{qp\mu_p(1+b)} - \frac{KT}{q}\,\frac{b-1}{b+1} \cdot \frac{1}{p}\,\frac{dp}{dx} - \frac{1}{q}\,\frac{d}{dx}\,\Delta E_g \qquad (2.12)$$

Thus, the voltage across I region can be found by integrating E in the base region.

$$V_I = \int_o^{W_n} E\,dx$$

$$= \int_o^{W_n} -\frac{J}{qp\mu_p(1+b)} \cdot dx + \int_o^{W_n} \frac{KT}{q} \cdot \frac{b-1}{b+1} \cdot \frac{1}{p} \cdot \frac{dp}{dx} + \int_o^{W_n} \frac{1}{q} \cdot \frac{d}{dx}\Delta E_g\, d$$

or

$$V_I = -\frac{J}{q\mu_p(1+b)} \int_o^{W_n} \frac{1}{p}\,dx + \frac{KT}{q}\,\frac{b-1}{b+1} \int_{P(o)}^{P(W_n)} \frac{1}{p}\,dp + \frac{1}{q}\int_{\Delta E_g(o)}^{\Delta E_g(W_n)} d\Delta E_g$$

$$V_I = -\frac{J}{q\mu_p(1+b)} \int_o^{W_n} \frac{1}{p}\,dx + \frac{KT}{q}\,\frac{b-1}{b+1}\,\ln\{P(W_n)\} - \ln\{p(o)\}$$

$$+ \frac{1}{q}(\Delta E_g(W_n) - \Delta E_g(o) \qquad (2.13)$$

The carrier concentration p in the middle region can be found using equation (2.7) and 2.8. From (2.8)

$$E + E_o = \frac{J_n}{qn\,\mu_n} - \frac{q}{q}\frac{D_n}{\mu_n}\cdot\frac{1}{n}\cdot\frac{dn}{dx}$$

with the help of eqn. (2.10) and (2.11), it can be written as

$$E + E_o = \frac{J_n}{qp\,\mu_n} - \frac{KT}{q}\,\frac{1}{p}\,\frac{dp}{dx}$$

on keeping it in eqn. (2.7)

$$J_p = qp\,\mu_p\left(\frac{J_n}{qp\,\mu_n} - \frac{KT}{q}\,\frac{1}{p}\,\frac{dp}{dx}\right) - q\,D_p\,\frac{dp}{dx}$$

$$J_p - \frac{\mu_p}{\mu_n}J_n = -\frac{KT}{q}\,q\,\mu_p\,\frac{dp}{dx} - q\,D_p\,\frac{dp}{dx}$$

$$J_p - \frac{1}{b}J_n = -2q\,D_p\,\frac{dp}{dx} \qquad (2.14)$$

On taking the derivative of above equation

$$\frac{dJ_p}{dx} - \frac{1}{b}\,\frac{dJ_n}{dx} = -2q\,D_p\,\frac{d^2p}{dx^2}$$

On combining this with equation (2.9)

$$-\frac{qp}{\tau} - \frac{1}{b}\,\frac{qp}{\tau} = -2q\,D_p\,\frac{d^2p}{dx^2}$$

or

$$\frac{d^2p}{dx^2} = \frac{1}{2qD_p}\,\frac{qp}{\tau}\left(\frac{1+b}{b}\right)$$

or

$$\frac{d^2p}{dx^2} = \frac{p}{L^2} \qquad (2.15)$$

where

$$L^2 = 2\, D_p \tau \left(\frac{b}{1+b}\right) \tag{2.16}$$

The solution of equation (2.15) is given by

$$P = A \cosh(x/L) + B \sinh(x/L) \tag{2.17}$$

where A and B are constants.

The boundary conditions can be found by assuming injection efficiency to be unity. Therefore,

$$\text{at} \quad x = 0 \qquad J_n = 0 \tag{2.18}$$

$$\text{and} \quad x = W_n \qquad J_p = 0 \tag{2.19}$$

With the help of equations(2.14), (2.18) and (2.19), the boundary conditions for (2.17) can be written

at $x = 0$ $\quad J_n = 0$, and $J_p = -2q\, D_p \frac{dp}{dx}$

$$\text{Therefore,} \quad J = -2q\, D_p \left.\frac{dp}{dx}\right|_{x=0} \tag{2.20}$$

$$\text{or} \quad \left.\frac{dp}{dx}\right|_{x=0} = -\frac{J}{2qD_p}$$

at $x = W_n$ $\quad J_n = 2qD_p \; b \frac{dp}{dx} \quad J_p = 0$

Therefore, $\quad J = 2q\, D_p\, b \left.\frac{dp}{dx}\right|_{x=W_n}$

or

$$\left.\frac{dp}{dx}\right|_{x=W_n} = \frac{J}{2.b.q.D_p} \tag{2.21}$$

on differentiating equation (2.17), we get

$$\frac{dp}{dx} = \frac{A}{L} \sinh(x/L) + \frac{B}{L} \cosh(x/L)$$

at $x = 0$,

$$\left.\frac{dp}{dx}\right|_{x=0} = \frac{A}{L} \sinh(0) + \frac{B}{L} \cosh(0)$$

From eqn. (2.20)

$$\frac{A}{L} \cdot 0 + \frac{B}{L} = - \frac{J}{2q D_p}$$

or

$$B = - \frac{J.L.}{2q D_p} \qquad (2.22)$$

at $x = W_n$,

$$\left.\frac{dp}{dx}\right|_{x=W_n} = \frac{A}{L} \sinh\left(\frac{W_n}{L}\right) + \frac{B}{L} \cosh\left(\frac{W_n}{L}\right)$$

From eqns. (2.21) and (2.22),

$$\frac{A}{L} \sinh\left(\frac{W_n}{L}\right) + \left(- \frac{J.L.}{2.q.D_p}\right) \frac{1}{L} \cosh\left(\frac{W_n}{L}\right) = \frac{J}{2bqD_p}$$

or

$$\frac{A}{L} \sinh\left(\frac{W_n}{L}\right) = \frac{J}{2bqD_p} + \frac{J}{2qD_p} \cosh\left(\frac{W_n}{L}\right)$$

or

$$A = \frac{J.L.}{2.q.D_p} \cdot \frac{1}{\sinh\left(\frac{W_n}{L}\right)} \left[\frac{1}{b} + \cosh\left(\frac{W_n}{L}\right)\right] \qquad (2.23)$$

Keeping the value of A and B from equations (2.22) and (2.23) into (2.17) we will get

$$p = \frac{J.L.}{2qD_p} - \frac{1}{\sinh(\frac{W_n}{L})} \left(\frac{1+b\cosh(W_n/L)}{b}\right) \cosh(x/L) - \frac{J.L.}{2qD_p} \sinh(x/L)$$

or

$$p = \frac{J.L.}{2qD_p} \left[\frac{1+b\cosh(W_n/L)}{b\sinh(W_n/L)} \cosh(x/L) - \sinh(x/L)\right]$$

or

$$p = \frac{J.L.}{2qD_p} \left[\frac{\cosh x/L + b\cosh(W_n/L)\cosh x/L - b\sinh(x/L)\sinh(W_n/}{b.\sinh(W_n/L)}\right.$$

or

$$p = \frac{J.L.}{2.q.D_p} \frac{1}{b\sinh(W_n/L)} [\cosh x/L + b\cosh(W_n-x)/L] \qquad (2.24)$$

Using the above equation, the carrier density in the base region is plotted in Figs. 2.3, 2.4 and 2.5 for different values of life time and forward current density.

To find V_I we have to integrate 1/p with respect to dx. The eqn. (2.24) can be rewritten as

$$p = \frac{J.L.}{2q D_p b\sinh(W_n/L)} \left[\frac{e^{x/L} + e^{-x/L}}{2} + b\left(\frac{e^{(W_n-x)/L} + e^{-(W_n-x)/L}}{2}\right)\right.$$

or

$$p = C\left[A\, e^{x/L} + B\, e^{-x/L}\right] \qquad (2.25)$$

where

$$C = \frac{J.L.}{2q D_p b\sinh(W_n/L)} \qquad (2.26)$$

$$A = \tfrac{1}{2} + \tfrac{1}{2} b\, e^{-W_n/L} \qquad (2.27)$$

$$B = \tfrac{1}{2} + \tfrac{1}{2} b\, e^{W_n/L} \qquad (2.28)$$

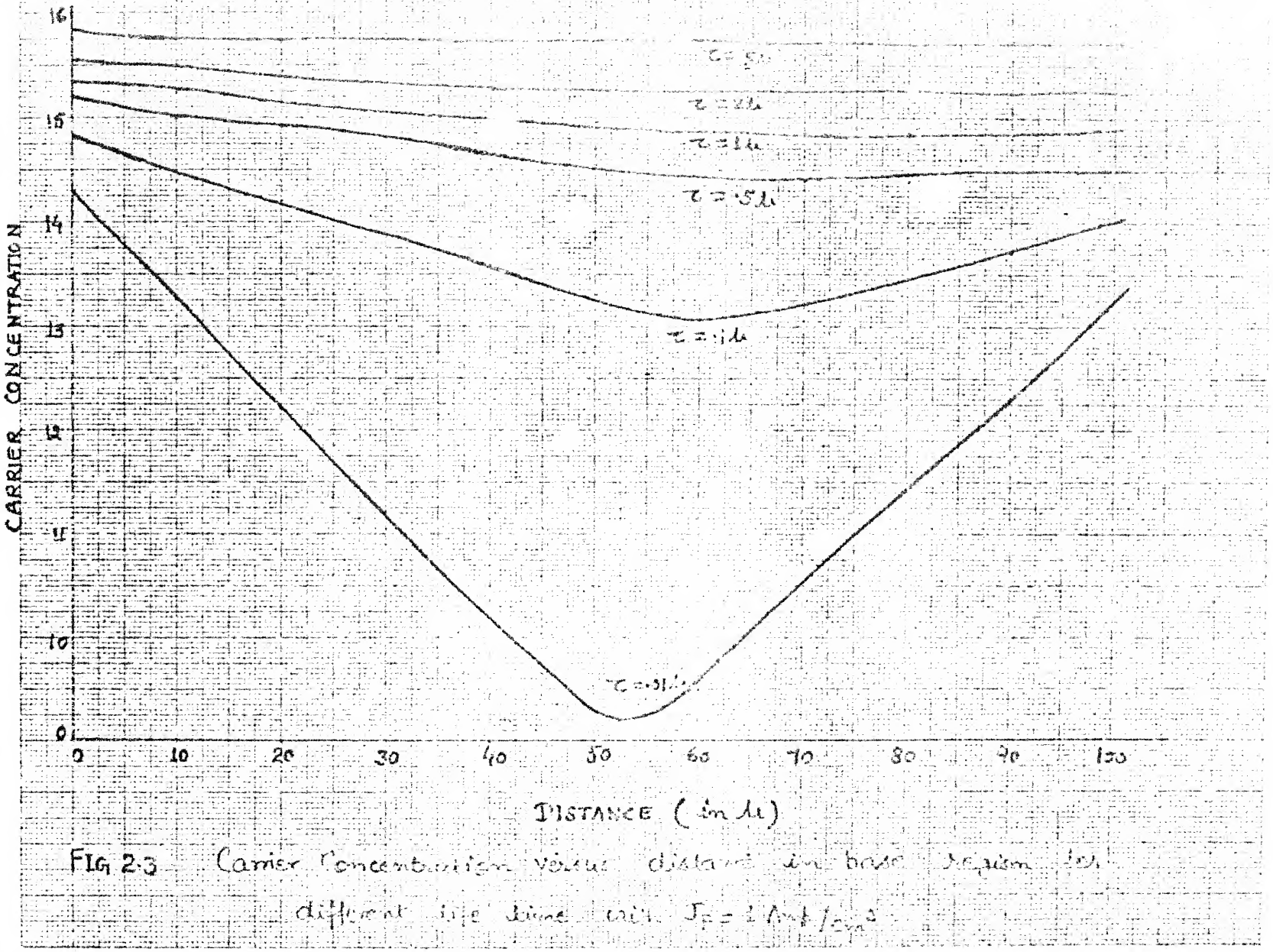

FIG 2.3 Carrier concentration versus distance in base region for different life time with $J_F = 2$ Amp/cm^2

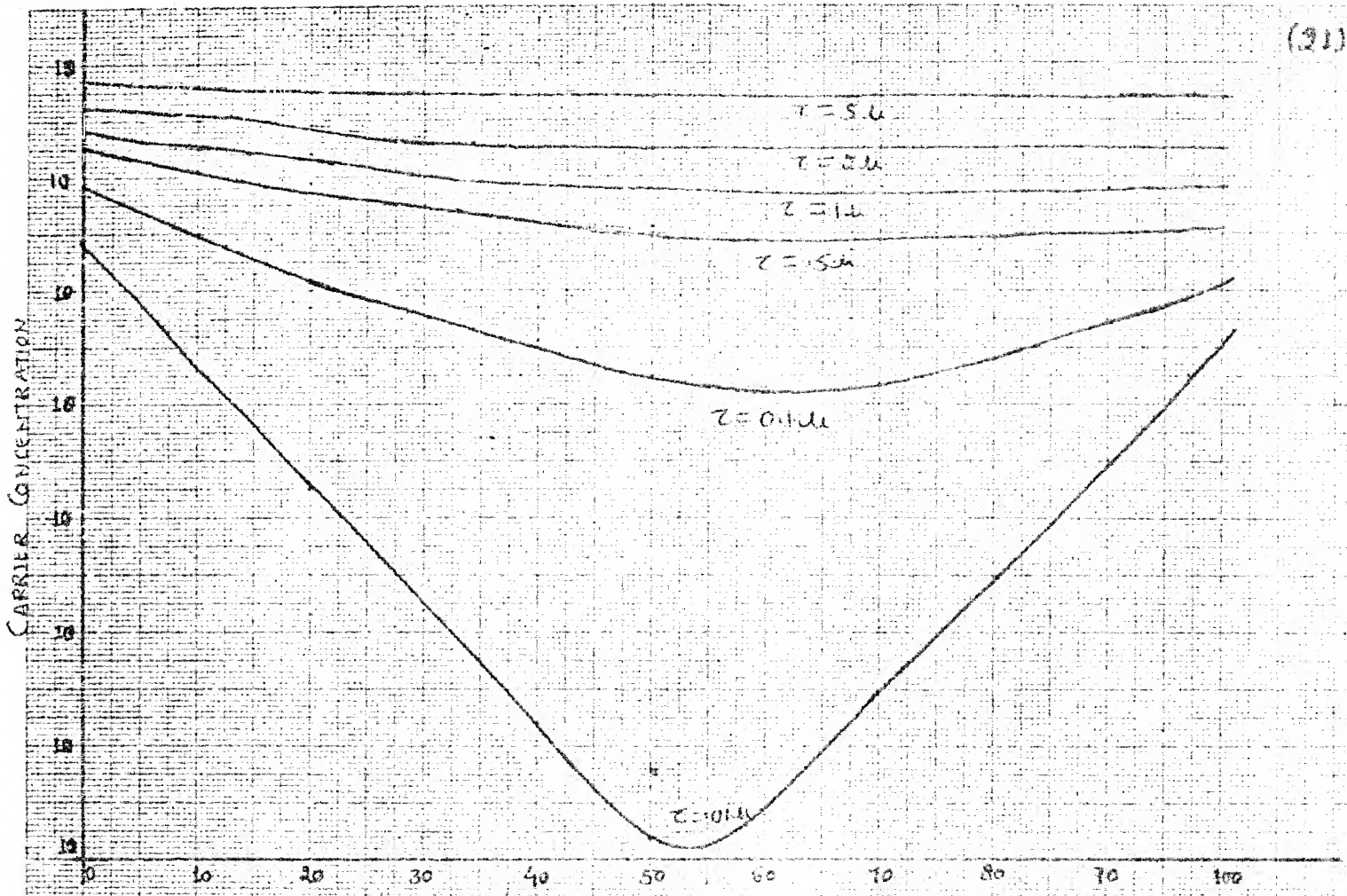

FIG 2.4

Carrier Concentration Vs distance in Base region for different life time with $J_E = 100$ A/cm^2

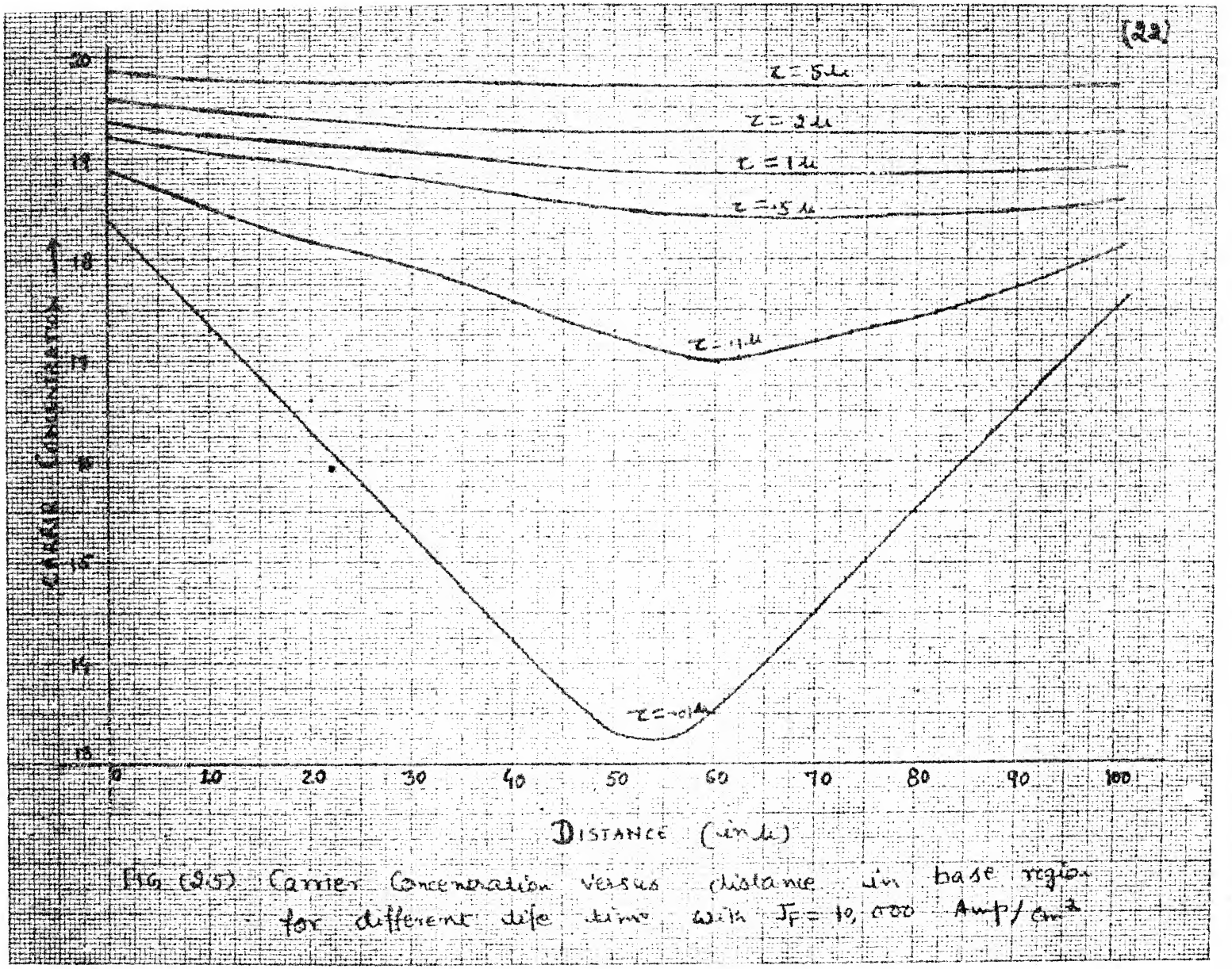

Fig (2.5) Carrier Concentration Versus distance in base region for different life time with $J_F = 10,000$ Amp/cm^2

Now,

$$\int_0^{W_n} \frac{1}{p}\,dx = \int_0^{W_n} \frac{1}{C\left[A\,e^{x/L} + B\,e^{-x/L}\right]}\,dx \qquad (2.29)$$

Since,

$$\int \frac{dx}{a\,e^{mx} + b\,e^{-mx}} = \frac{1}{m\sqrt{ab}} \cdot \tan^{-1}\left(e^{mx}\sqrt{\frac{a}{b}}\right) \qquad (2.30)$$

Put $x/L = Y$ and $dx = L\,dy$ in equation (2.29)

$$\int_0^{W_n} \frac{1}{p}\,dx = \int_0^{W_n/L} \frac{L\,dy}{C(A\,e^{y} + B\,e^{-y})} \qquad (2.31)$$

In analogy to eqn. (2.30), eqn. (2.31) can be written as

$$\int_0^{W_n} \frac{1}{p}\,dx = \frac{L}{C}\left[\frac{1}{\sqrt{AB}}\tan^{-1}\left\{e^{y}\sqrt{\frac{A}{B}}\right\}\right]_0^{W_n/L}$$

or

$$= \frac{L}{C\sqrt{AB}}\left[\tan^{-1}\left\{e^{W_n/L}\sqrt{\frac{A}{B}}\right\} - \tan^{-1}\left\{e\sqrt{\frac{A}{B}}\right\}\right]$$

or

$$\int_0^{W_n} \frac{1}{p}\,dx = \frac{L.2q\,D_p\,b\,\sinh(W_n/L)}{J.L.\sqrt{\left\{\left(\frac{1}{2} + \frac{1}{2}\,b\,e^{W_n/L}\right)\left(\frac{1}{2} + \frac{1}{2}\,b\,e^{-W_n/L}\right)\right\}}}$$

$$\left[\tan^{-1}\left\{e^{W_n/L}\sqrt{\frac{\frac{1}{2} + \frac{1}{2}\,b\,e^{W_n/L}}{\frac{1}{2} + \frac{1}{2}\,b\,e^{W_n/L}}}\right\} - \tan^{-1}\left\{\sqrt{\frac{\frac{1}{2} + \frac{1}{2}\,b\,e^{-W_n/L}}{\frac{1}{2} + \frac{1}{2}\,b\,e^{-W_n/L}}}\right\}\right] \qquad (2.32)$$

Combining eqns. (2.13), (2.21) and (2.32), V_I can be written as

$$V_I = -4 \frac{KT}{q} \frac{b}{1+b} \frac{\sinh W_n/L}{\{b^2 + 2b \cosh(W_n/L) + 1\}^{\frac{1}{2}}} [\tan^{-1}\{e^{W_n/L} \sqrt{\frac{1+b\, e^{-W_n/L}}{1+b\, e^{W_n/L}}}\} -$$

$$\tan^{-1}\{\sqrt{\frac{1+b\, e^{-W_n/L}}{1+b\, e^{W_n/L}}}\}] + \frac{KT}{q} \left(\frac{b-1}{b+1}\right) \ln \left[\frac{b+\cosh(W_n/L)}{b\cosh(W_n/L)+1}\right]$$

$$+ \frac{1}{q} [\Delta E_g (W_n) - \Delta E_g(0)] \qquad (2.33)$$

Now the voltage across P^+-N and N-N^+ junction can be found using Boltzmann law for junctions which states that if $\bar{P}$ is the thermal equilibrium carrier concentration and P is the carrier concentration after a voltage V_a is applied across junction then

$$P = \bar{P}. \exp(\frac{qV_a}{KT})$$

or

$$V_a = \frac{KT}{q} \cdot \ln (P/\bar{P})$$

Let, V_L be the voltage drop across left junction and V_R be across right junction.

also $\bar{p}(x)$: is the thermal equilibrium hole concentration in n region

$p(x)$: is the equilibrium hole concentration after the voltage is applied.

Now, the voltage across left and right junctions is

$$V_L = \frac{KT}{q} \ln \frac{p(0)}{\bar{p}(0)} \qquad (2.34)$$

$$V_R = \frac{KT}{q} \ln \frac{n(W_n)}{\bar{n}(W_n)} \tag{2.35}$$

V Combining equations (2.34), (2.35) and (2.10)

$$V_L + V_R = \frac{KT}{q} \ln \frac{p(0).\ p(W_n)}{p(0).\ \bar{n}(W_n)}$$

Since n region is constantly doped. Therefore, in thermal equilibrium

$$\bar{n}\ \bar{p} = n_i^2$$

$$V_L + V_R = \frac{KT}{q} \ln \frac{p(0).\ p(W_n)}{n_i^2} \tag{2.36}$$

On calculating $p(0).\ p(W_n)$ from equation (2.24)

$$p(0).\ p(W_n) = \{ \frac{J.L.}{2q\ D_p\ b \sinh(W_n/L)} \}^2 \{(b \cosh(W_n/L) + 1\}^{x} \{ b + \cosh(W_n/L)\}$$

$$p(0).\ p(W_n) = C^2 \ .\ J^2$$

where

$$C^2 = \{ \frac{L}{2q\ D_p\ b \sinh(W_n/L)} \}^2 \{ b \cosh(W_n/L) + 1\} \{ b + \cosh(W_n/L) \} \tag{2.37}$$

Therefore,

$$V_L + V_R = \frac{KT}{q} \ . \ln(\frac{C^2\ J^2}{n_i^2})$$

or

$$= \frac{2KT}{q} \ln(\frac{CJ}{n_i}) \tag{2.38}$$

The total voltage drop across the diode is the sum of the voltages across left junction, base region and right junction

$$\therefore \quad V_A = V_L + V_R + V_I$$

or

$$V_L + V_R = V_A - V_I \tag{2.39}$$

Using eqn. (2.38)

$$\frac{2KT}{q} \ln \left(\frac{CJ}{n_i}\right) = V_A - V_I$$

Therefore,

$$J = -\frac{n_i}{C} e^{qV_A/2KT} \cdot e^{-qV_I/2KT} \tag{2.40a}$$

$$J = J_s \exp\left(\frac{qV_a}{2KT}\right) \tag{2.40b}$$

where $J_s = -\frac{n_i}{C} e^{-qV_I/2KT}$

and C, V_I are given by equations (2.37) and (2.33) respectively.

2.3.2 At high Currents

So far, we have assumed unit injection efficiency. But as the current is increased, the end region currents can not be neglected. Herlet [7] has considered the end region currents also. Instead of boundary conditions given by equations (2.17) and (2.18), he has assumed the following boundary conditions

$$J_n(-d) = \eta_l J \tag{2.41}$$

$$J_p(+d) = \eta_r J \tag{2.42}$$

$$J_m = \eta_m J \tag{2.43}$$

As the sum of the three components is equal to the total current, the magnitude of η_l, η_r and η_m are related with each other by the relation

$$\eta_l + \eta_m + \eta_r = 1 \tag{2.44}$$

With these boundary conditions, Herlet has derived a theory for J-V relationship which at low currents could be approximated by the Halls theory. At high currents it gives the following relationship

$$J_F = \frac{\sqrt{b}}{(b+1)} \cdot \frac{(S+1)^2}{S} \cdot \left(\frac{q\, n_i\, 2D_p}{(1+b)\, L}\right)^2 \cdot \frac{1}{\sqrt{J_{ps}}\sqrt{J_{ms}}} \cdot \tanh^2\left(\frac{W_n}{2L}\right) \frac{J_F}{J}\left(\frac{J_F}{J} - 1\right) \tag{2.45}$$

where J_F is the total forward current, and J is the current due to the recombination in the middle region.

The voltage across the base region (in which the end region currents are significant) is given by

$$V_M = \frac{J_F}{J} V_M \tag{2.46}$$

where

$$V_M = -\frac{4KT}{q} \frac{b}{1+b} \frac{\sinh W_n/L}{\{b^2 + 2b\cosh(W_n/L) + 1\}^{\frac{1}{2}}} \left[\tan^{-1}\left\{e^{W_n/L} \frac{\sqrt{1+b}\, e^{-W_n/L}}{1+b\, e^{W_n/L}}\right\} + \tan^{-1}\left\{\sqrt{\frac{1 + b\, e^{-W_n/L}}{1 + b\, e^{W_n/L}}}\right\}\right] \tag{2.47}$$

which is only the first term of equation (2,33). Actually, in the derivation of V_I, due to the assumption of unit injection

efficiency, J in the first term has been cancelled out. Otherwise a multiplication factor J_F/J will come. This factor, being nearly equal to unity, could be deleted at low currents. But at high currents J_F/J increases and makes the first term so high that the other terms in equation (2.33) can be neglected.

For arbitrary doping profile the currents in the P and N regions, can be written as

$$J_n = \frac{q D_n}{\int_0^{W_p} N_A/n_i^2 \, dx} \exp\left(\frac{qV_a}{KT}\right) \qquad (2.48a)$$

$$J_o = \frac{q D_p}{\int_0^{W_n} N_D/n_i^2 \, dx} \exp\left(\frac{qV_a}{KT}\right) \qquad (2.48b)$$

where W_p and W_n are the widths of the P and N regions respectively and V_a is the applied voltage.

In P^+ N N^+ diode, therefore, the electron current in P^+ region will be

$$J_{nP} = \frac{q D_n}{\int_{-W_p}^{0} N_A(x)/n_{ie}^2 \, dx} \exp\left(\frac{qV_L}{KT}\right) \qquad (2.49)$$

and the hole current in the n^+ region will be

$$J_{pN} = \frac{q D_p}{\int_{W_n}^{W_{nn}} N(x)/n_{ie}^2 \, dx} \exp\left(\frac{qV_R}{KT}\right) \qquad (2.50)$$

where nie for the heavily doped region is given in equation (2.50).

If long (means base region width longer than the diffusion length) P^+ and N^+ regions are involved, then equations (2.49) and (2.50) will be modified to take into account the minority carrier diffusion length. The decay in the current density can be approximated by an exponential function. Therefore, for only N^+ and P^+ regions, equation (2.49) and equation (2.50) will be modified as

$$J_{np} = J_{ns} \exp\left(\frac{qV_L}{KT}\right) \tag{2.51a}$$

where

$$J_{ns} = \frac{q D_n}{\int_{-W_p}^{o} \frac{N_A(x)}{n_{ie}^2} \exp\left(-\frac{x}{L_n}\right) dx} \tag{2.51b}$$

and

$$J_{pN} = J_{ps} \cdot \exp\left(\frac{qV_R}{KT}\right) \tag{2.52a}$$

where

$$J_{ps} = \frac{q D_p}{\int_{W_n}^{W_{nn}} \frac{N_D(n)}{n_{ie}^2(x)} \exp\left(-\frac{x}{L_p}\right) dx} \tag{2.52b}$$

The total voltage drop across the diode will be the sum of the voltage drops across left junction, middle region and the right junction. The sum of junction voltage drops could be approximated by the diffusion voltage across the two space

charge regions.

Thus, with the help of equations (2.45) to (2.47), (2.51) and (2.52), the J-V characteristics could be calculated. The forward J-V characteristics of PIN diode using equation (2.40) and the above equations is plotted for different values of life time in Fig. 2.6 to Fig. 2.12. In the Figures 2.6 to 2.11, Lanyon and Tuft's formula of band gap narrowing is used while in Figures 2.12 to 2.17 Slotboom's formula is used.

2.4 RESULTS AND DISCUSSIONS

From Figures 2.3, 2.4 and 2.5 it is clear that the carrier density is maximum at the two ends of the base regions and minimum, somewhere in between. The concentration at the two ends is different due to difference in the mobility of electrons and holes. The minimum of the carrier density changes with life time. At life time greater than about 1 μ sec. the carrier density is almost constant because of the low recombination rate. For life time less than 1 μ sec, a minima in carrier concentration occurs, since due to small life time, the diffusion length becomes small and hence the carriers get recombine before crossing the base region. The plots of different currents are identical. The only difference being in the magnitude of the carrier concentration, which increases with current.

Table 2.1 shows that when the reduction in band gap is considered, the J-V characteristics does not change appreciably

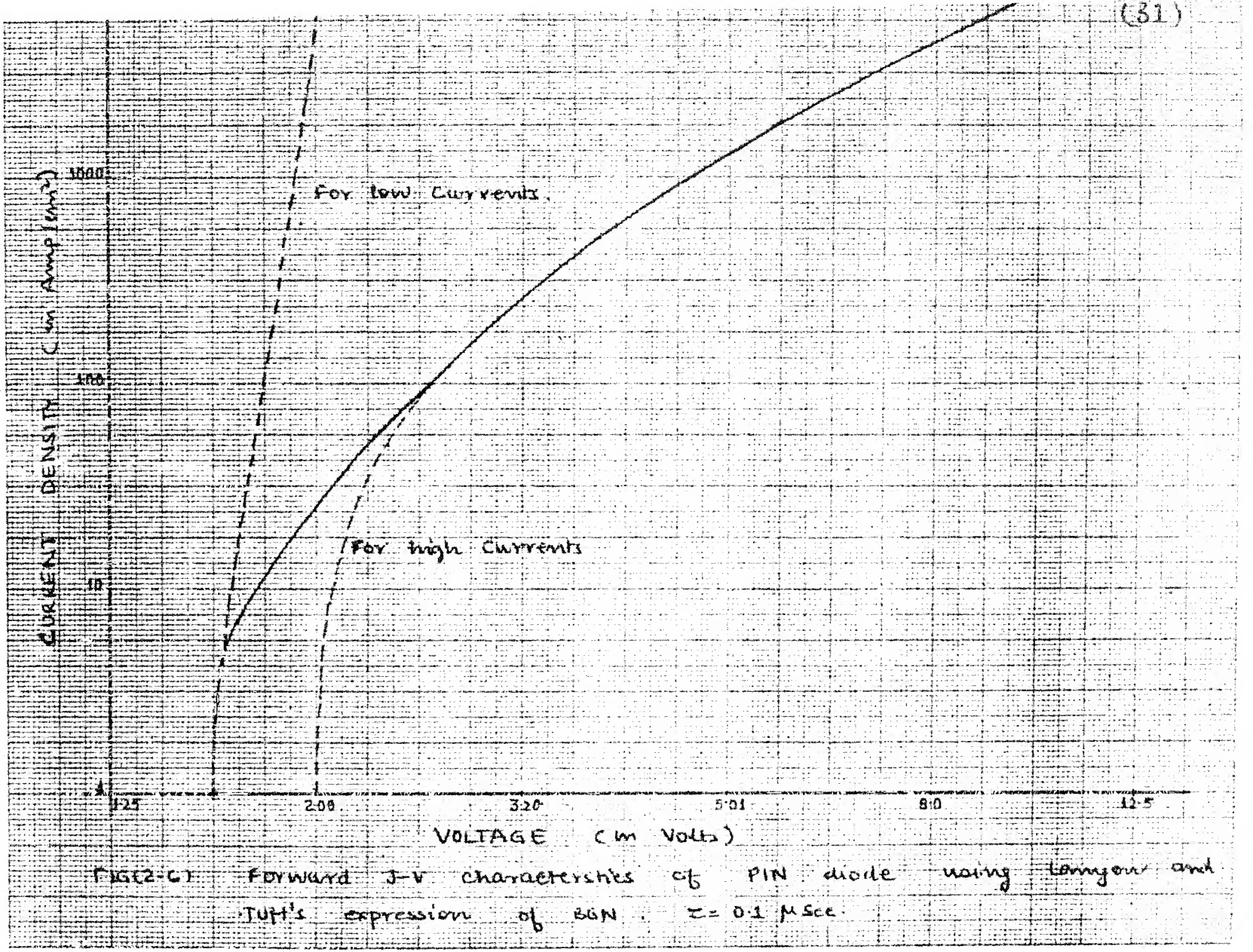

FIG(2-C) Forward J-V characteristics of PIN diode using Lampson and Tuft's expression of BGN. $\tau = 0.1\ \mu Sec$.

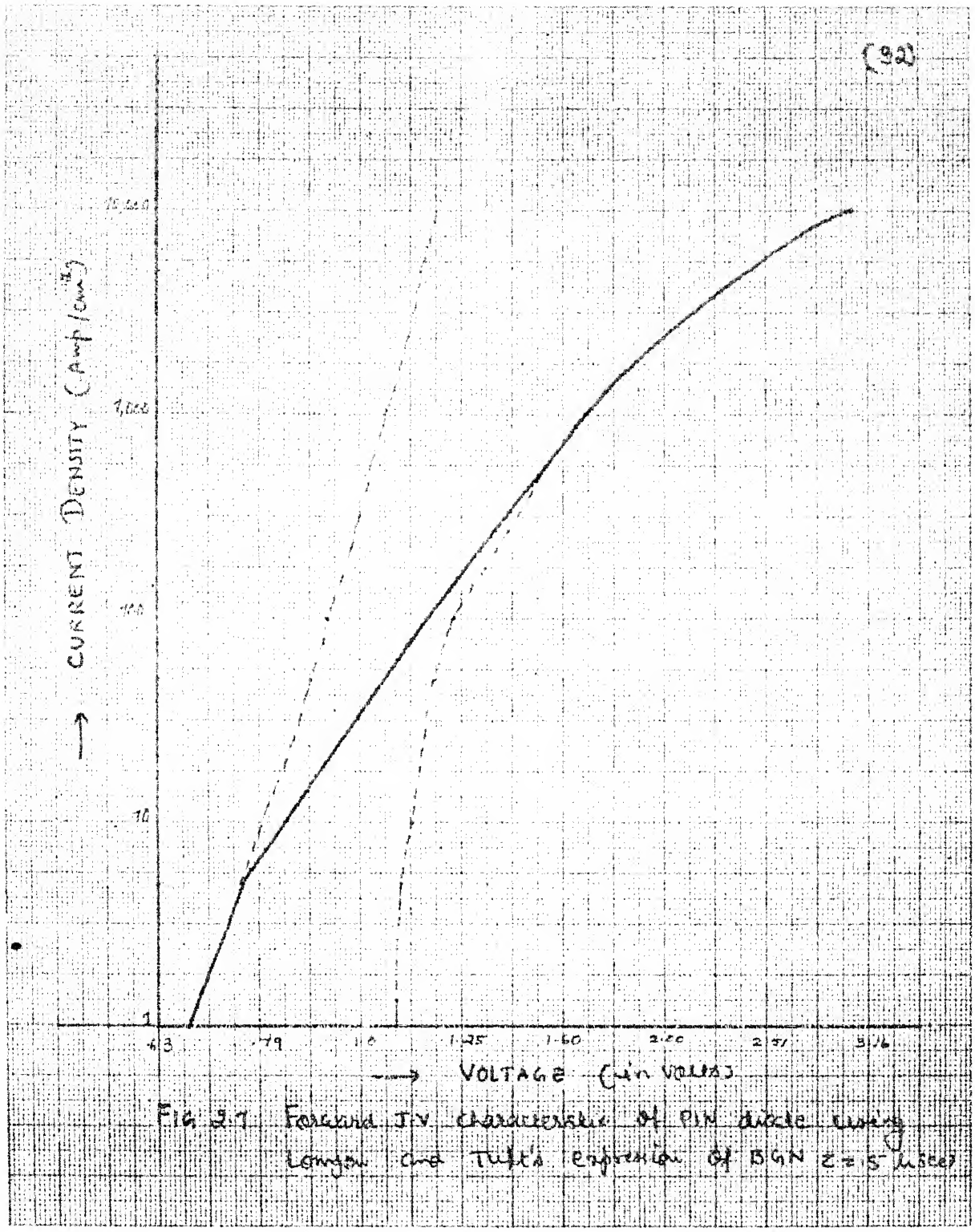

Fig 2.7 Forward I-V characteristic of PIN diode using Longini and Tufte's expression of BGN $E_g = 5$ used

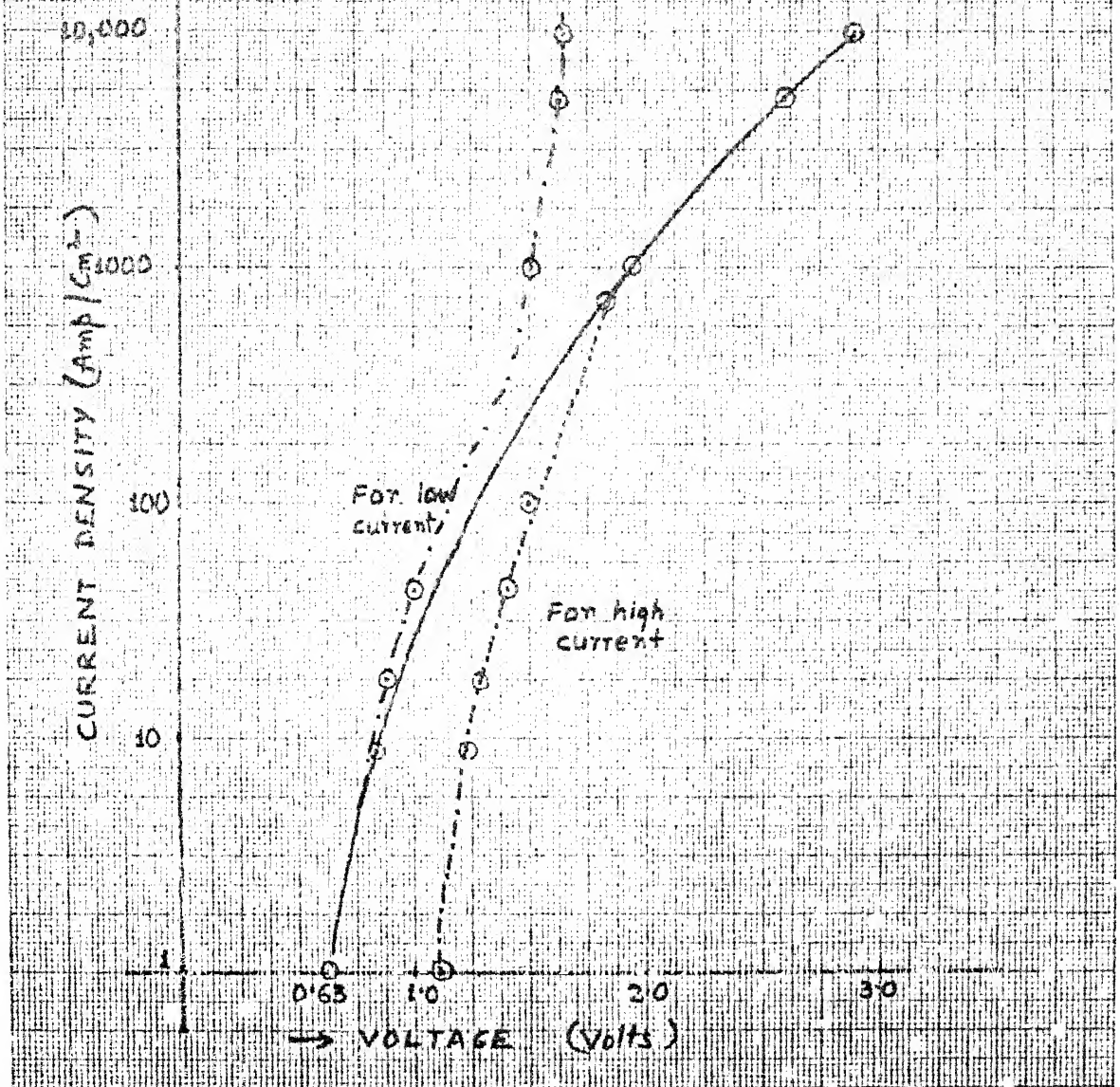

FIG. 2.8 : Forward J-V characteristics of PIN diode using Lanyon and Tuft's expression of BGN. $\tau = 1.5\,\mu$ sec.

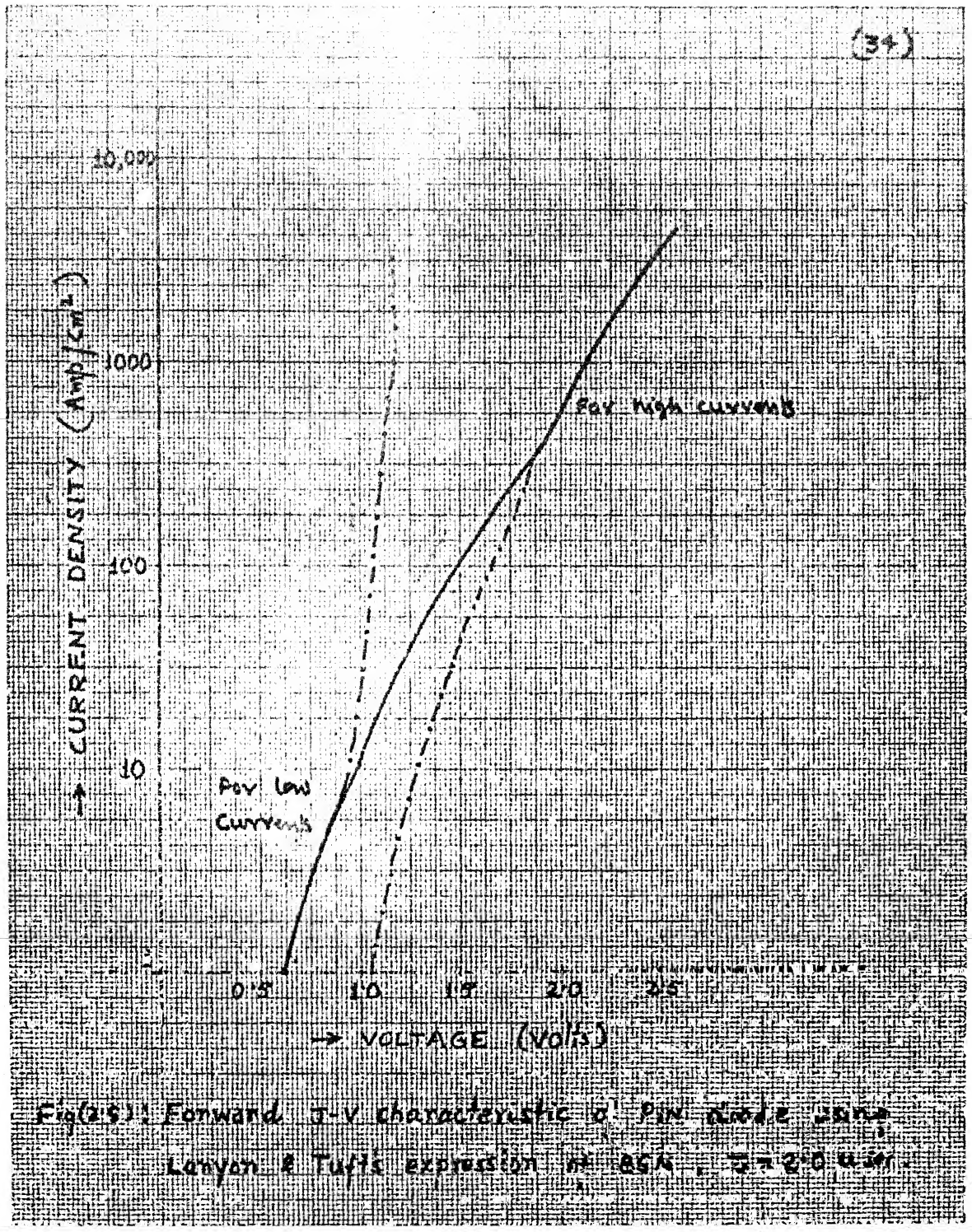

Fig(2·5): Forward I-V characteristic of p-n diode using Lanyon & Tuft's expression at 85°C, T = 2·0 μsec.

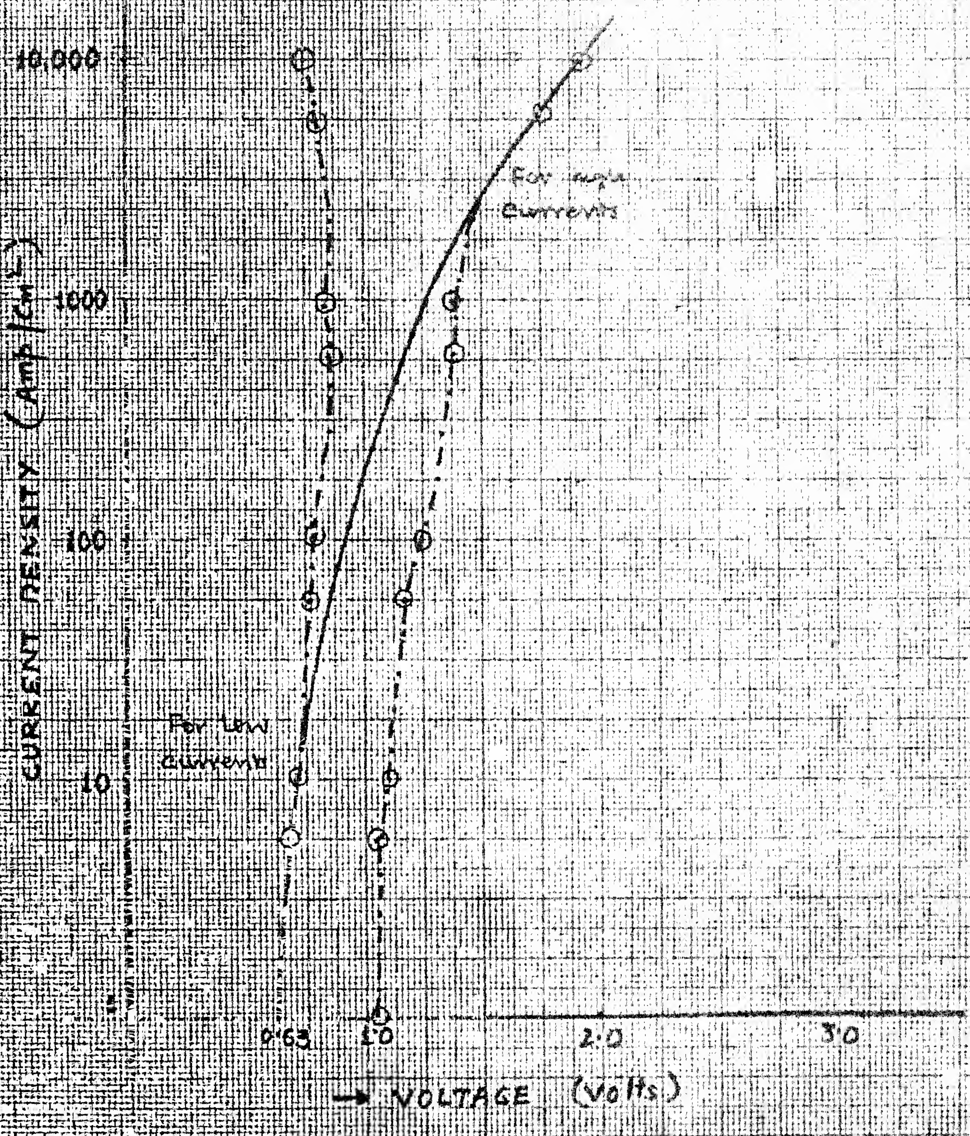

Fig 2.10 Forward J-V characteristics of PIN diode using Lanyon and Tuft's expression of ΔE_N $T = 300\,K$

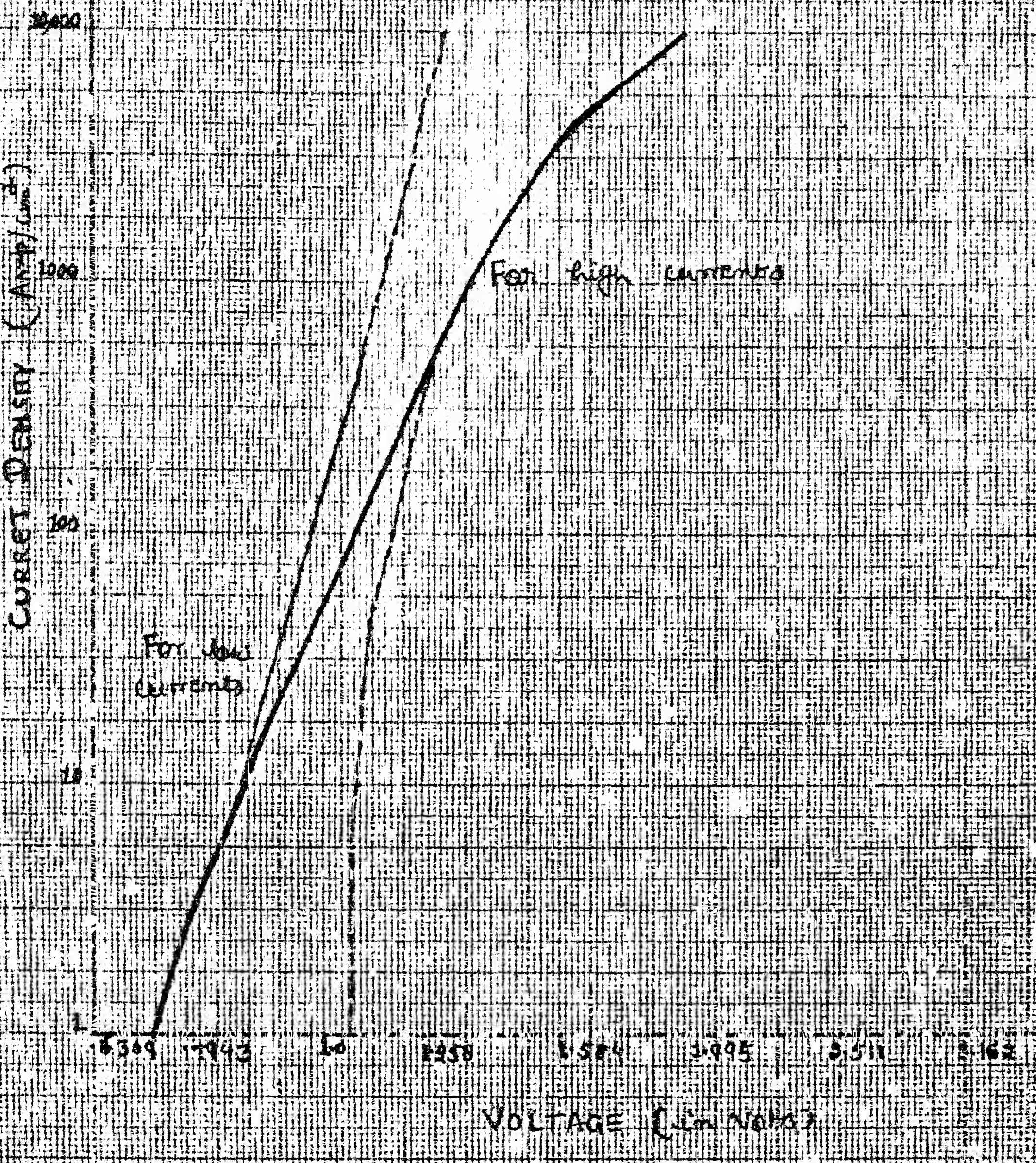

Fig (5.11) Forward I-V characteristics of p-n diode using Langon and Tuft's expression of BaN τ=10 sec

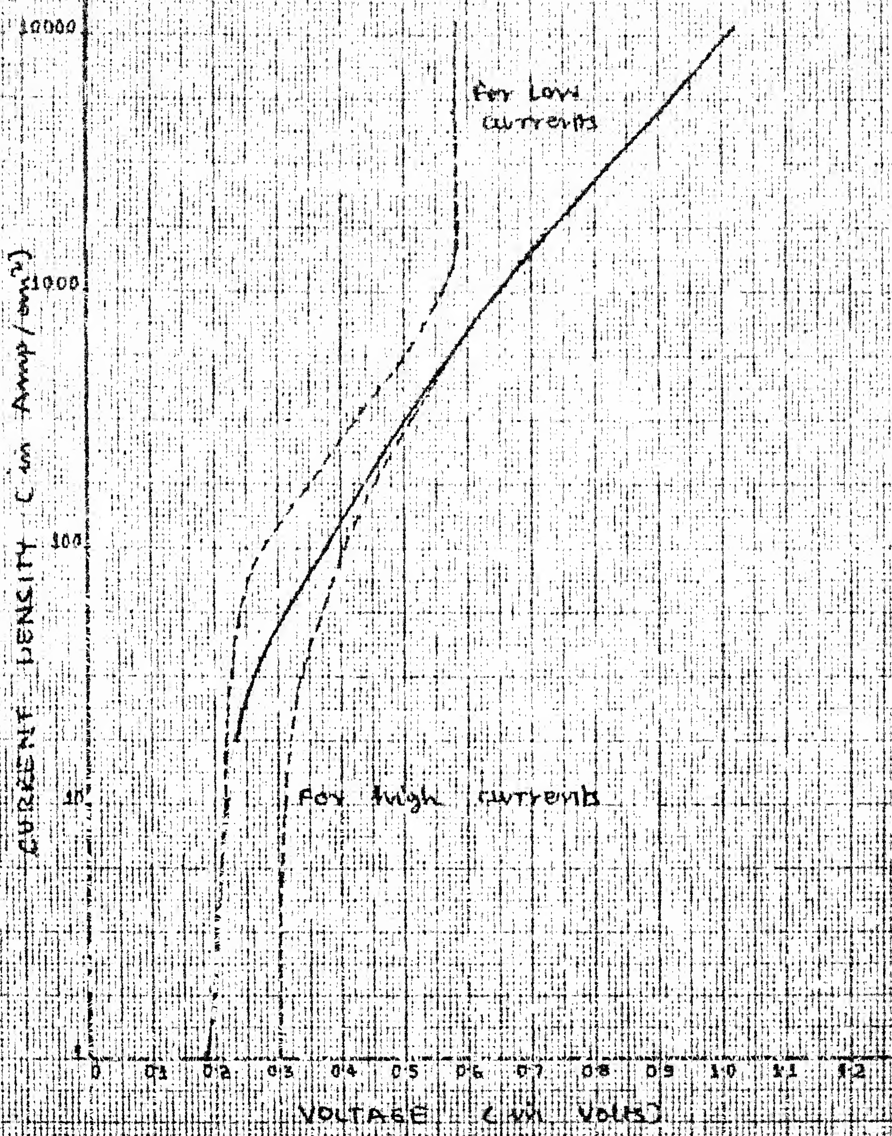

FIG (2.12) Forward J-V characteristics of PIN diode using Slotboom's expression of BGN. $\tau = 0.1\ \mu sec$.

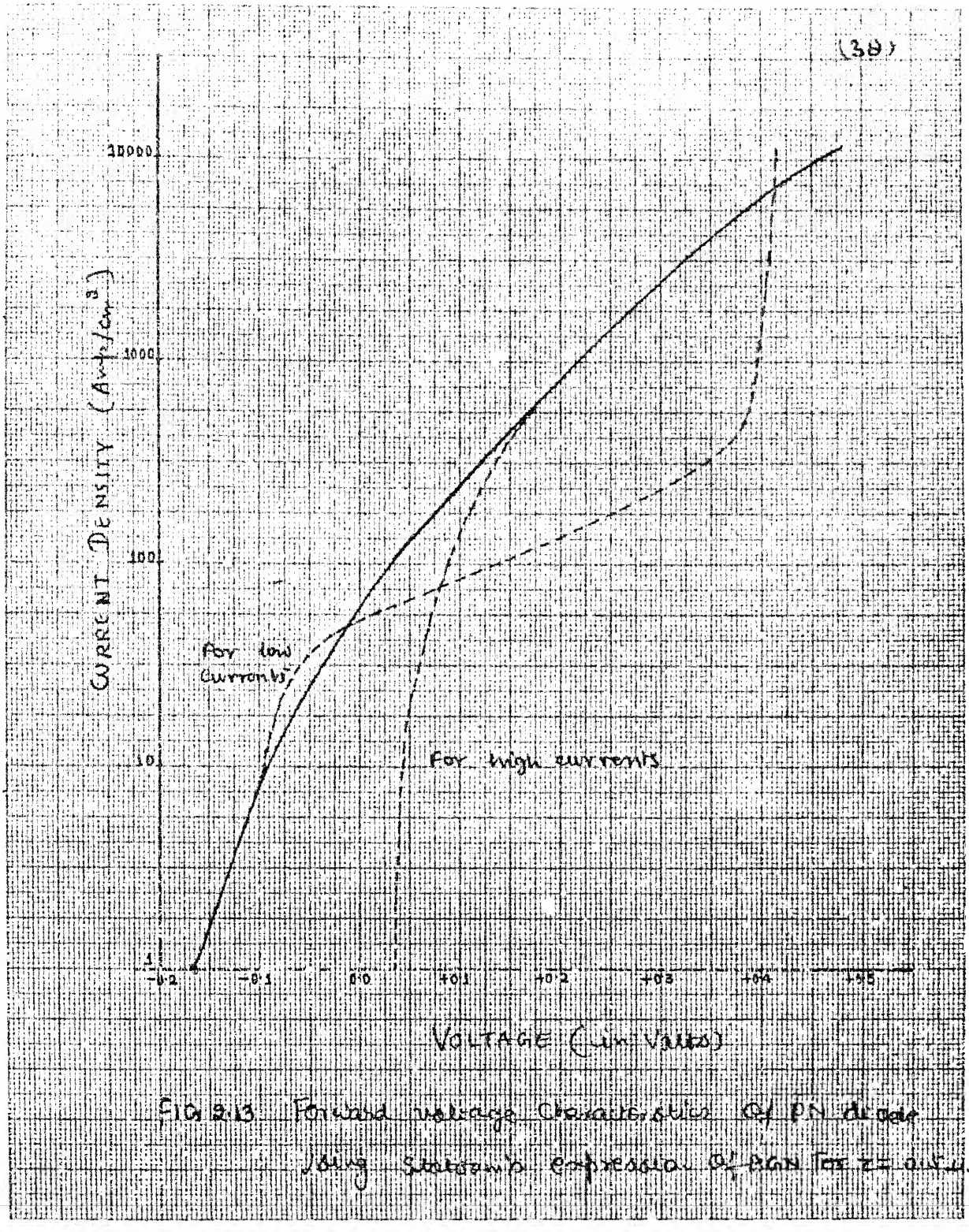

FIG 2.13 Forward voltage Characteristics of PN diode using Shockley's expression of PGN for $z = 0, L_p$

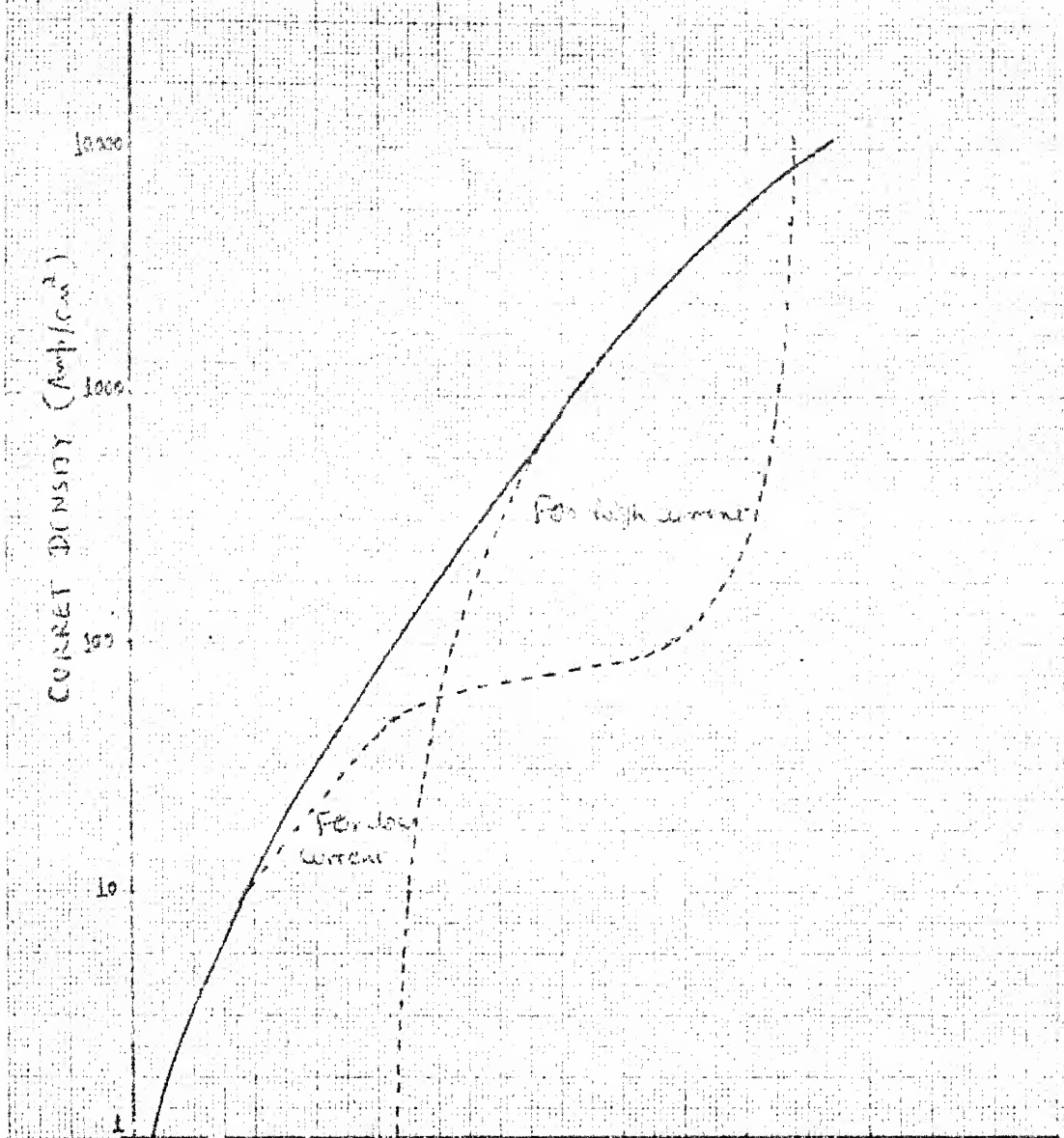

Fig 2·14 Forward I-V characteristic of PIN diode using Shockley's expression of BGN - $\tau = 1.0\mu Sec$

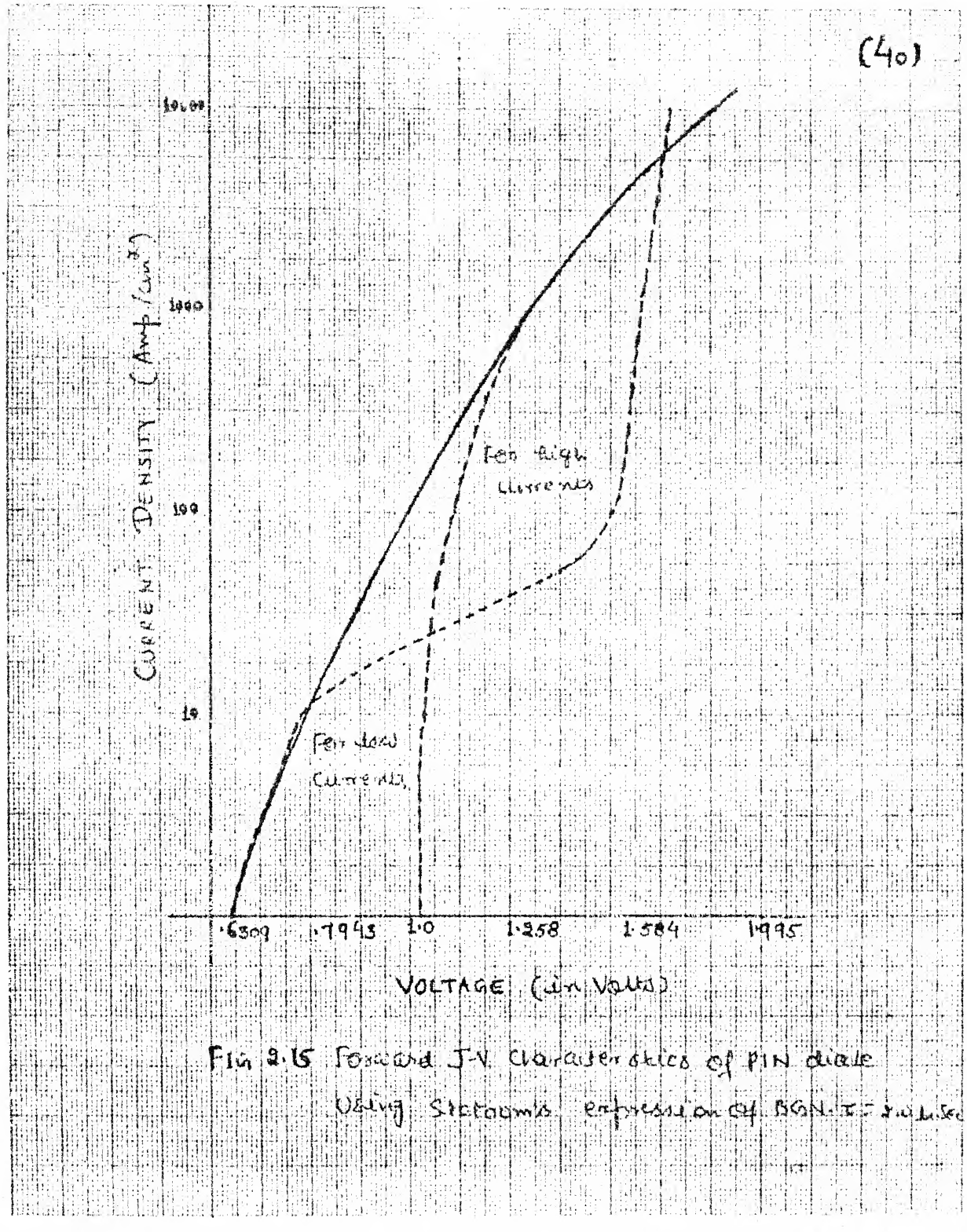

Fig 2.15 Forward J-V characteristics of PIN diode using Shockley's expression of BANDIT

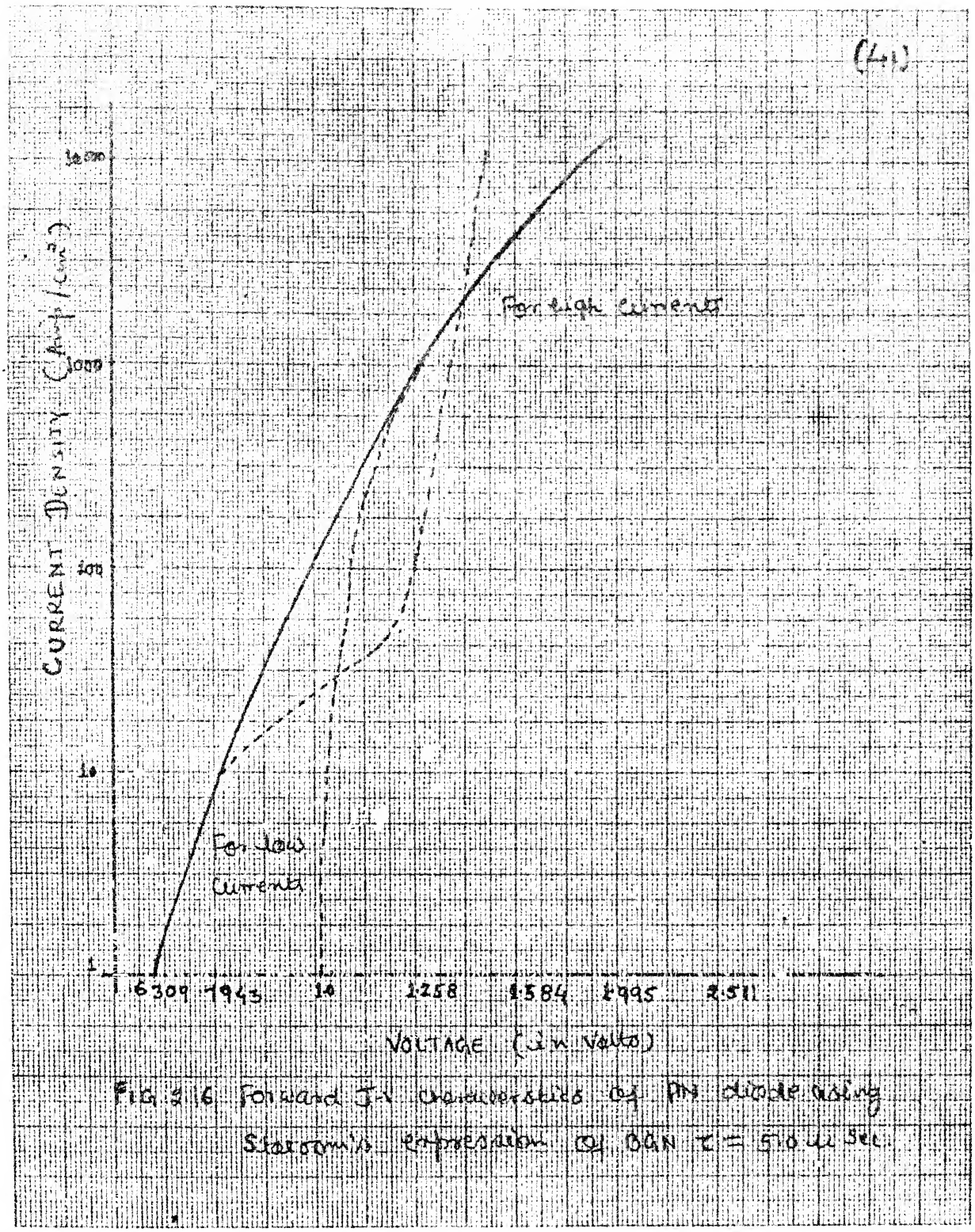

FIG 3.16 Forward I-V characteristics of PN diode using Shockley's expression of DAN τ = 5·0 μ Sec

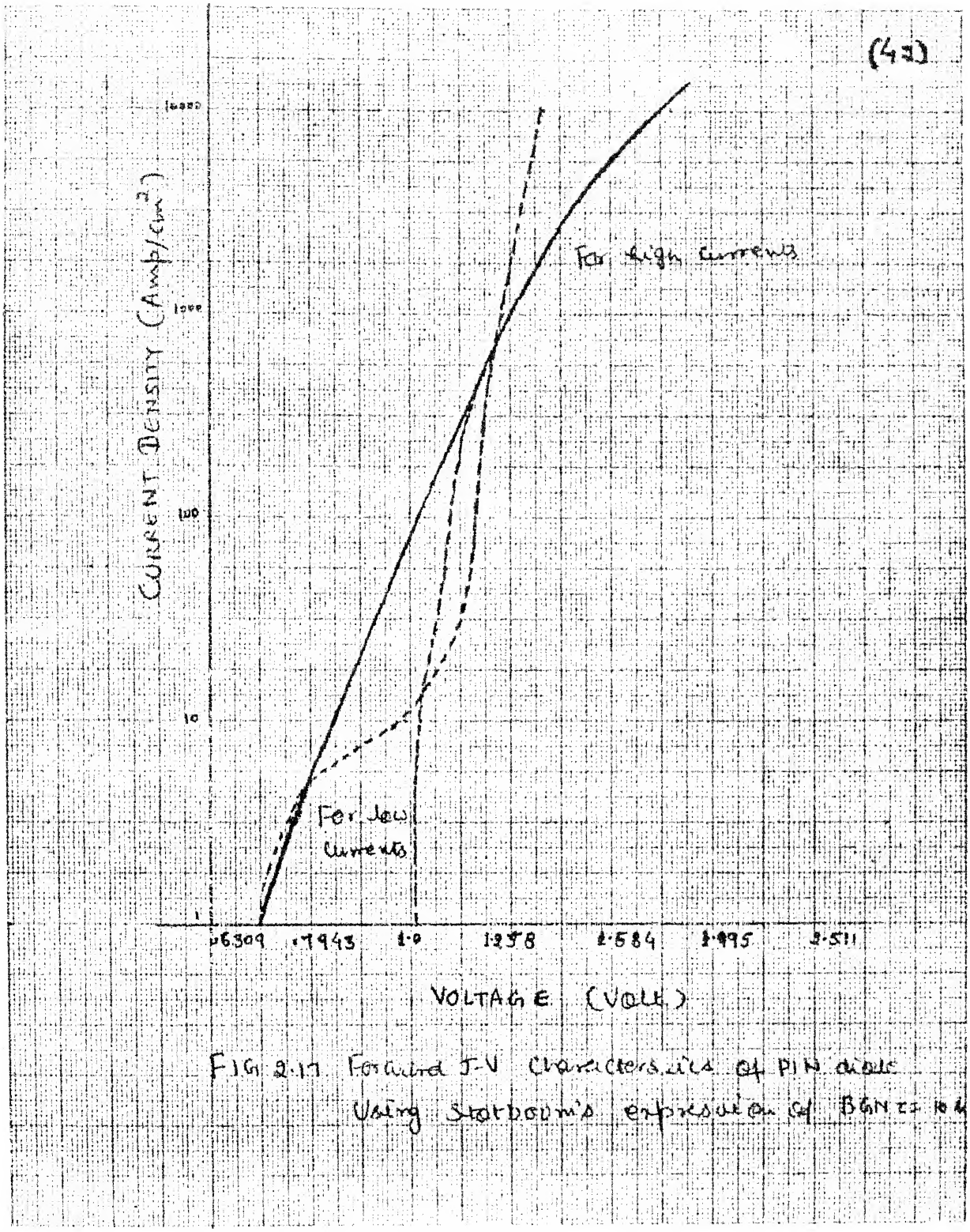

FIG 2.17 Forward I-V characteristics of PIN diode
Using Statbourn's expression of $B\tau_i = 10\,\mu sec$

Table 2.1 Forward I-V Characteristics at Low Currents Using Different Expressions of BGN

Current density (A/cm^2)	Voltage across PIN without considering BGN(Volts)	Voltage across PIN with Lanyon's expression(Volts)	Voltage across PIN with slot Slotboom's expression(Volts)
	τ = 0.1 μsec.		
1	1.539	1.539	1.539
5	1.622	1.623	1.622
10	1.658	1.659	1.658
50	1.741	1.743	1.742
100	1.777	1.780	1.781
	τ = 1 μsec.		
1	0.652	0.652	0.652
5	0.735	0.735	0.735
10	0.770	0.772	0.771
50	0.853	0.856	1.013
100	0.889	0.893	1.724

at low currents. While at high currents, band gap reduction modifies the J-V characteristics as could be seen from Fig. 2.18 where voltage and current density is plotted for both the case i.e. with band gap narrowing effect considered and without considering its effect. This is due to the fact that at lower currents band gap narrowing, which is occuring in the base region only due to high carrier concentration, is very small. At higher currents the heavily doped regions are also coming in the picture, in which band gap is reduced considerably due to high impurity concentration. This alters the saturation current density significantly, which in turn affect the J-V characteristics.

The voltage drop across PIN diode at higher current densities is high, for low values of life time. But as the life time increases beyond 1 μ sec. the voltage becomes nearly constant. To understand the variation of voltage with life time it is plotted in Figures 2.19 and 2.20 for low current densities and Figs. 2.21 and 2.22 for high current densities. The two plots of low current densities in which different formulae for band gap narrowing and the other two of high current densities are similar in nature. The voltage reaches a minimia at low currents for certain value of life time. Beyond this value of life time, the voltage again starts increasing. This is because, as the life time in the base region is increased, the carrier concentration in the base is also increased. This has the well known

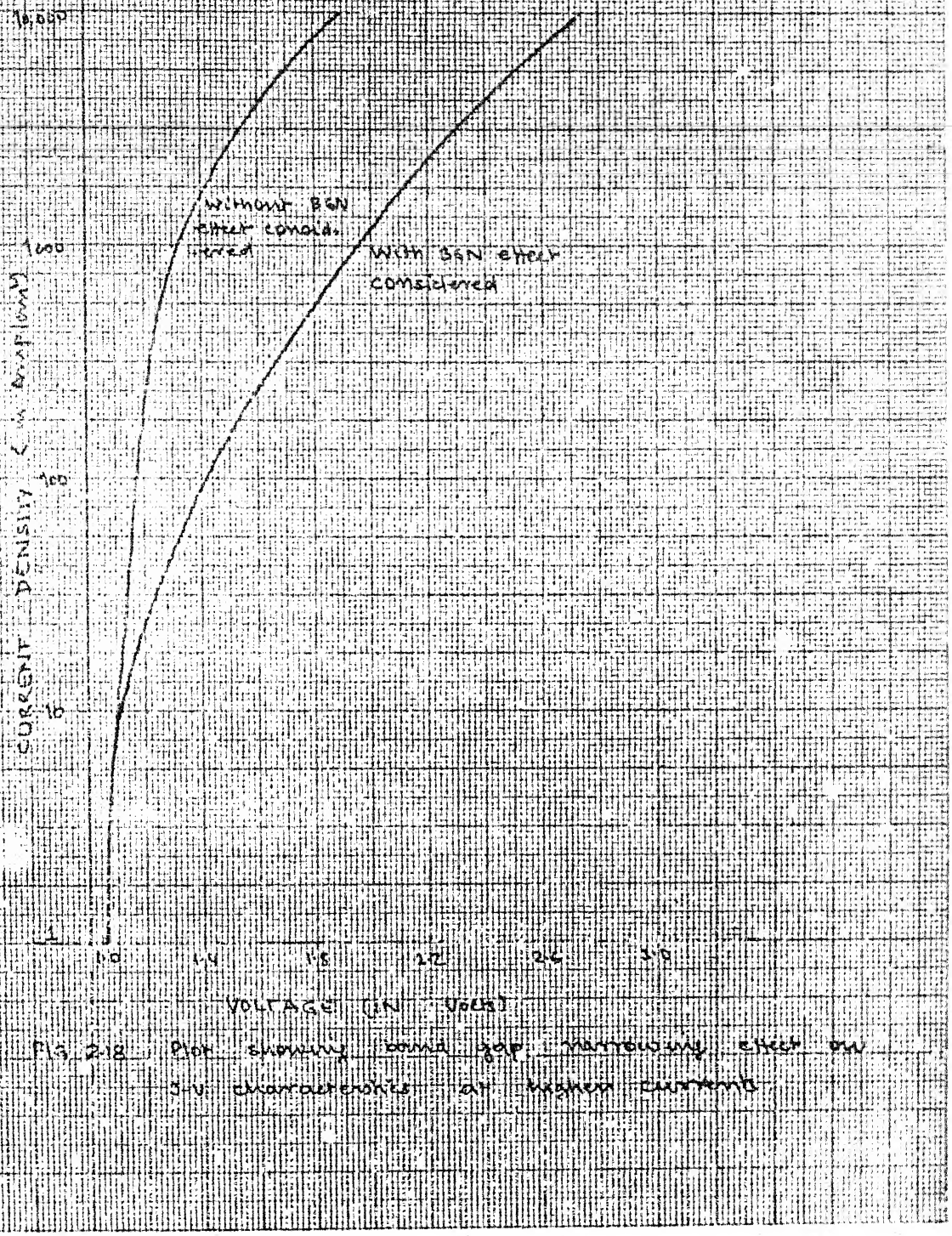

Fig 2.18 Plot showing band gap narrowing effect on I-V characteristics at maximum current

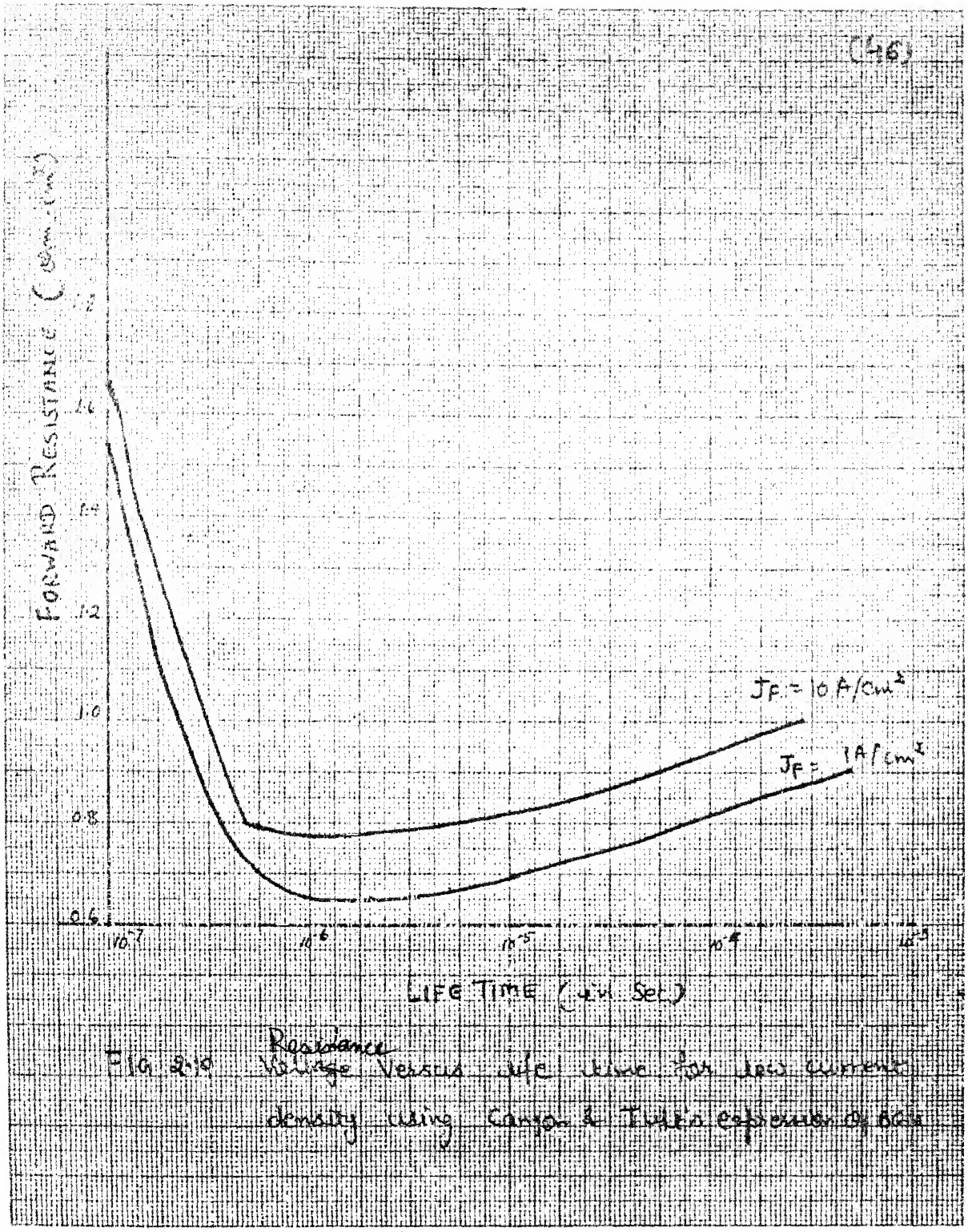

FIG 2.10 Resistance Voltage Versus Life time for two current density using Conyn & Tuller's expression of R_{ON}

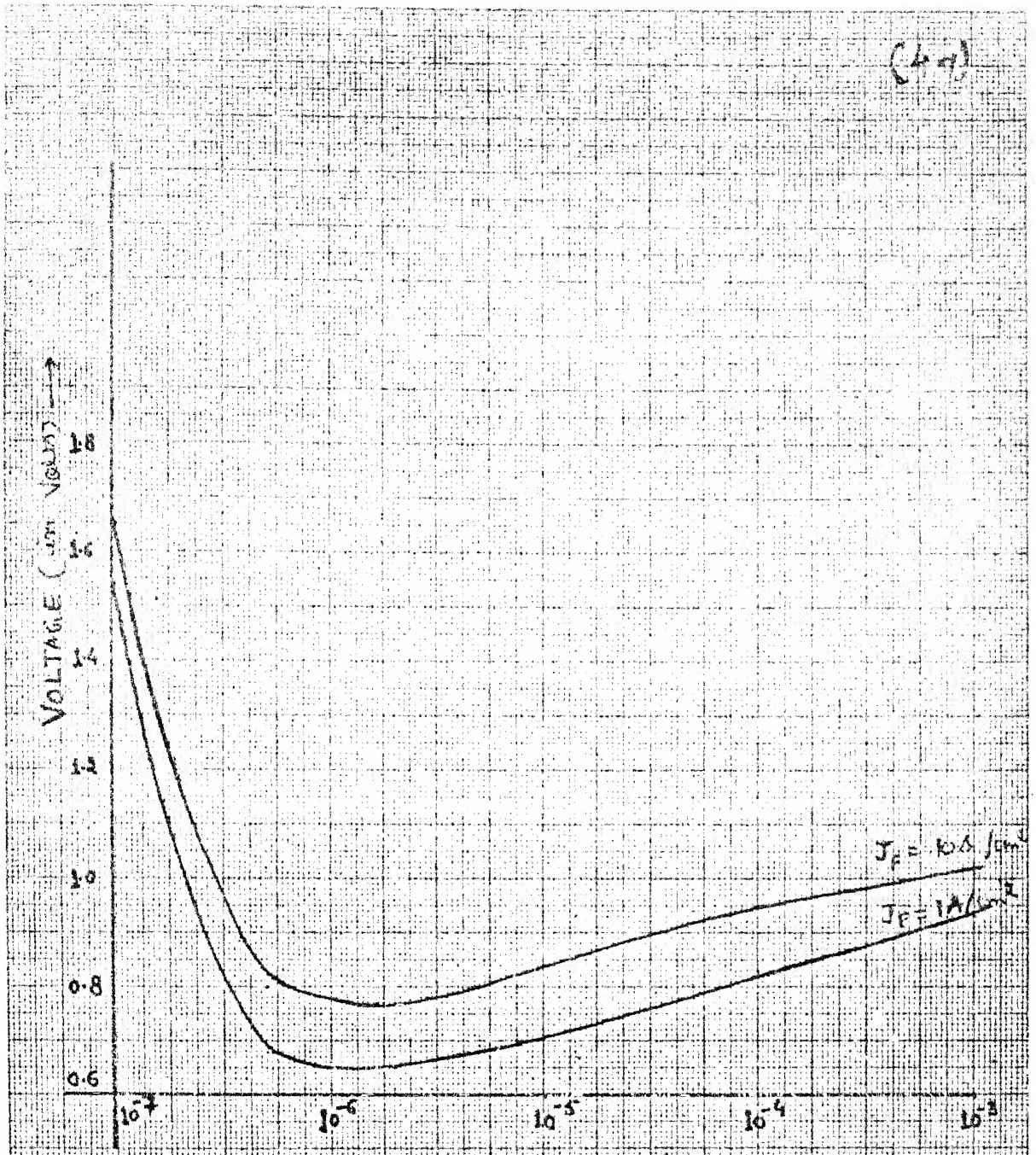

FIG (2.20) Voltage Versus life for low current density using Skarboom's of BGN

effect of enhancing the conductivity modulation and thereby reducing the voltage across the base region. However, in order to support a large carrier concentration at the edges of base region. The junction voltage must be raised as required by equation (2.36). Therefore, increasing the carrier life time is useful as long as base voltage forms a significant portion of the applied voltage. After the value of life time at which the base voltage becomes so small that it is negligible compared to junction voltage, an increase in life time will increase the junction voltage.

At higher current densities, instead of minima, the voltage becomes constant after a certain value of life time, which is plotted in Figures 2.21 and 2.22. To understand the reasoning, observe that for large values of life time the recombination current in the base region is very small and therefore the total forward current will be determined by, J_n and J_p (the end region currents). Herlet [17] has shown that at higher currents the total voltage drop across the diode is proportional to the square root of the current. Since the total current is constant, therefore, the voltage drop across PIN diode is also constant.

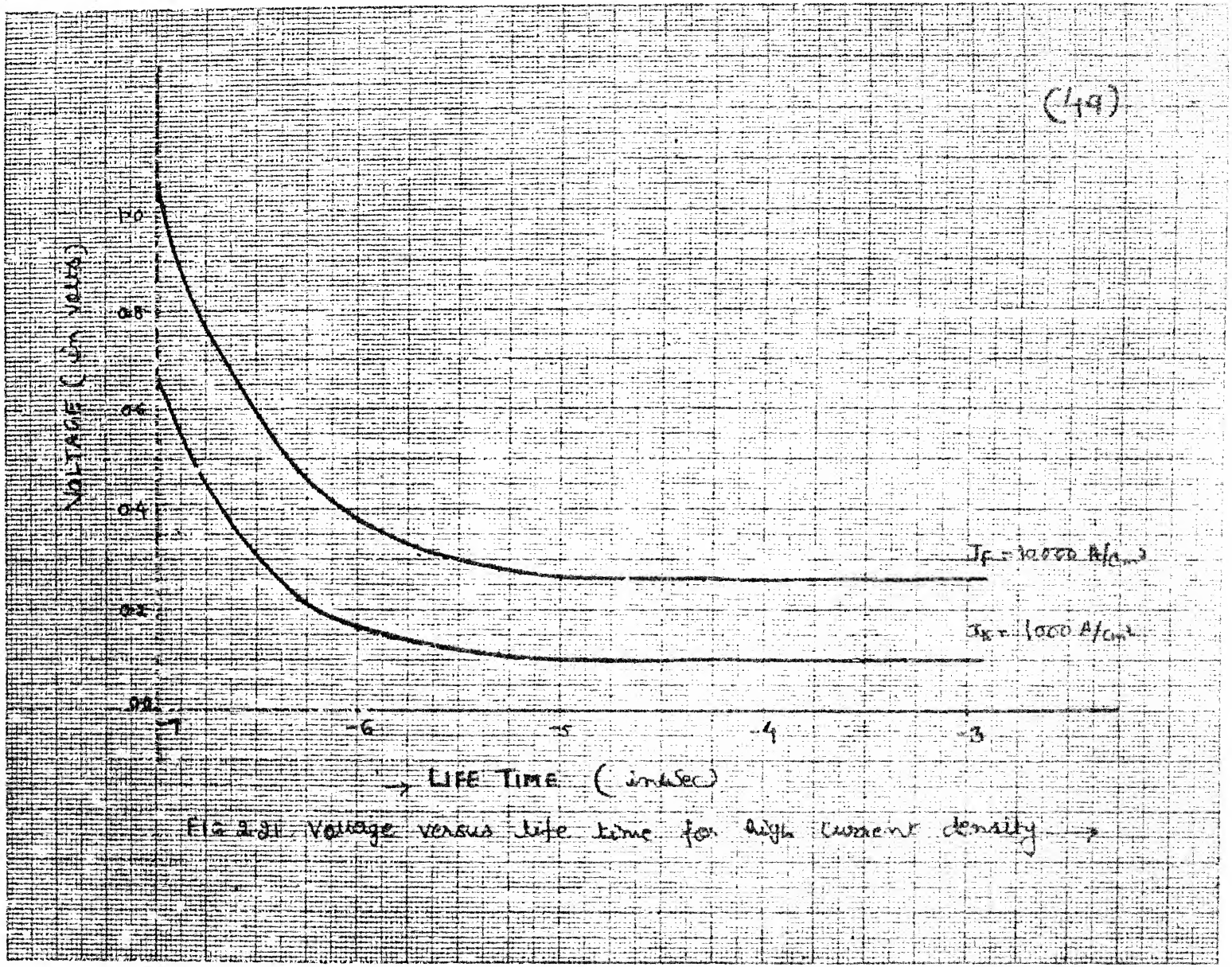

Fig 2.21 Voltage versus life time for high current density →

Fig 2.21

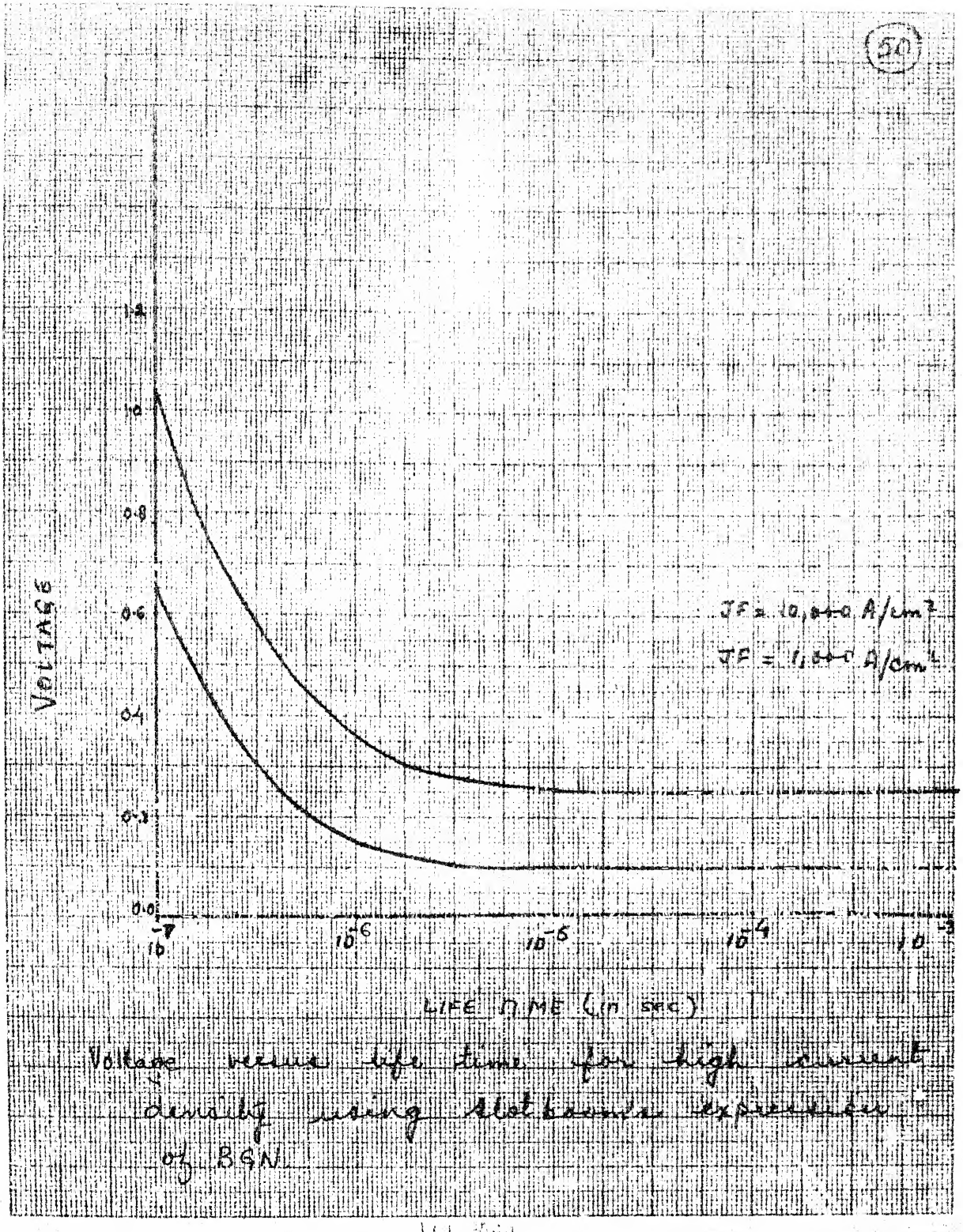

Voltage versus life time for high current density using Alot beam expander of BGN

CHAPTER 3

FORWARD RESISTANCE OF PIN DIODE

The forward J-V characteristics, discussed in the last chapter, are helpful in calculating forward resistance of the PIN diode. The forward resistance, beside fixing the isolation/insertion loss (depending upon whether the diode is shunt or series connected), as a function of current is an important parameter in the use of PIN diode as variolossers, amplitude modulation etc. In the present chapter the effect of various parameters on the dependence of forward resistance on current is discussed.

3.1 EFFECT OF BAND GAP NARROWING

The total forward resistance of PIN diode consists of contact resistance, resistance of the heavily doped regions and the base region resistance. At low currents the base region resistance is generally very high as compared to the other components. Therefore, the total forward resistance at low currents consists of base resistance only. As the current is increased, the base region is flooded with more and more charge carriers, which will decrease its resistance. At higher currents, therefore, the total forward resistance will consist of the contact resistance and the resistance of the heavily doped regions, the base resistance being negligibly small.

The base region resistance of the PIN diode can be calculated using the forward voltage drop across the base region, which is given by equation (2.33) and is rewritten here.

$$V_I = 4\frac{kT}{q}\frac{b}{1+b}\frac{\sinh(W_n/L)}{\{b^2+2b\cosh(W_n/L)+1\}^{\frac{1}{2}}}$$

$$\left[\tan^{-1}\left\{e^{W_n/L}\sqrt{\frac{1+b\exp(-W_n/L)}{1+b\exp(W_n/L)}}\right\}\right.$$

$$\left.-\tan^{-1}\left\{\sqrt{\frac{1+b\exp(-W_n/L)}{1+b\exp(W_n/L)}}\right\}\right]-\frac{1}{q}\left[\Delta E_g(W_n)-\Delta E_g(o)\right]$$

$$-\frac{KT}{q}\frac{b-1}{b+1}\ln\left[\frac{b\cosh(W_n/L)+1}{\{b\cosh(W_n/L)+1\}}\right]$$

In this equation, the last term is the voltage due to the diffusion current. If this term is delted the remaining will give the product of the forward resistance and current. Dividing by the current density, we will get

$$R_F A = \frac{4}{J}\frac{kT}{q}\frac{b}{(1+b)}\frac{\sinh(W_n/L)}{\{b^2+2b\cosh(W_n/L)+1\}^{\frac{1}{2}}}$$

$$\left[\tan^{-1}\left\{\sqrt{\frac{1+b\exp(-W_n/L)}{1+b\exp(W_n/L)}}\right\}-\tan^{-1}\left\{\sqrt{\frac{1+b\exp(-W_n/L}{1+b\exp(W_n/L)}}\right\}\right]$$

$$-\frac{1}{J}\frac{1}{q}\left[\Delta E_g(W_n)-\Delta E_g(0)\right] \qquad (3.1)$$

Using equation (3.1), forward resistance in Ω cm^2 is plotted in Fig. 3.1 with band gap narrowing being considered as well as without being considered. The plot is linear if band gap narrowing is not considered (since log of forward resistance is plotted against log of forward current density). When band gap narrowing is considered, the forward resistance at higher currents increases. This is because, at higher currents, the carrier concentration in the base region increases, which will increase the band gap narrowing and hence, the forward resistance will increase. The forward resistance as a function of current is again plotted in Fig. 3.2 for a higher value of life time (τ = 10.0 μ sec). At higher life time the average carrier concentration in the base region increases which will increase the band gap narrowing. Now, a greater deviation from linearily is expected, which is in fact the case as can be seen from Fig. 3.2.

3.2 EFFECT OF MATERIAL PARAMETERS ON FORWARD RESISTANCE

3.2.1 Base width effect

In order to find out the effect of base width, forward resistance is plotted as a function of base width for different values of current, in Figs. 3.3 and 3.4. The forward resistance increases with increase in the base width, the increase being rapid at higher base widths. The forward resistance is further plotted with respect to current for different base widths in Figs. 3.5 and 3.6. The figure shows

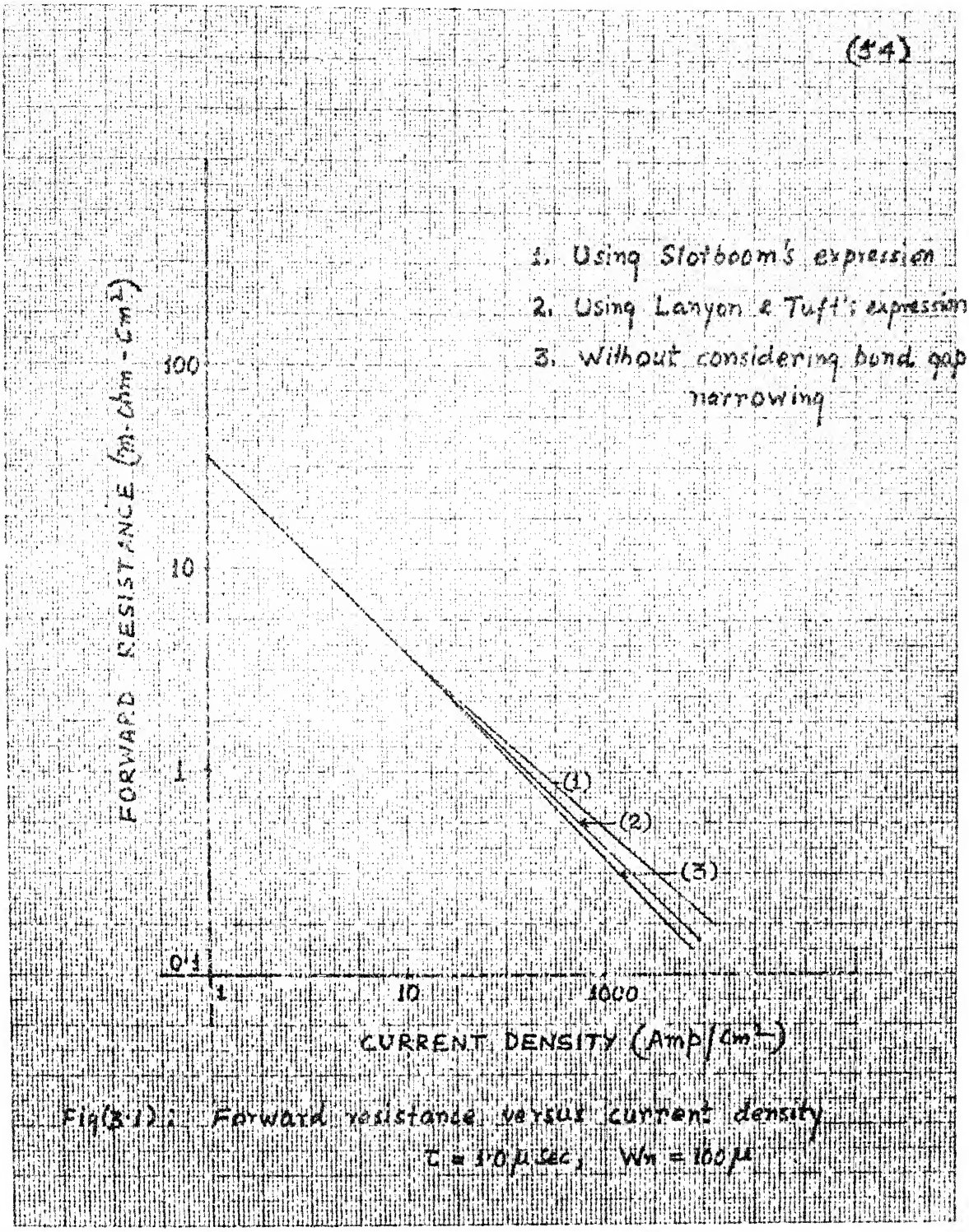

Fig(3.1): Forward resistance versus current density
$\tau = 1.0\,\mu$ sec, $W_n = 100\,\mu$

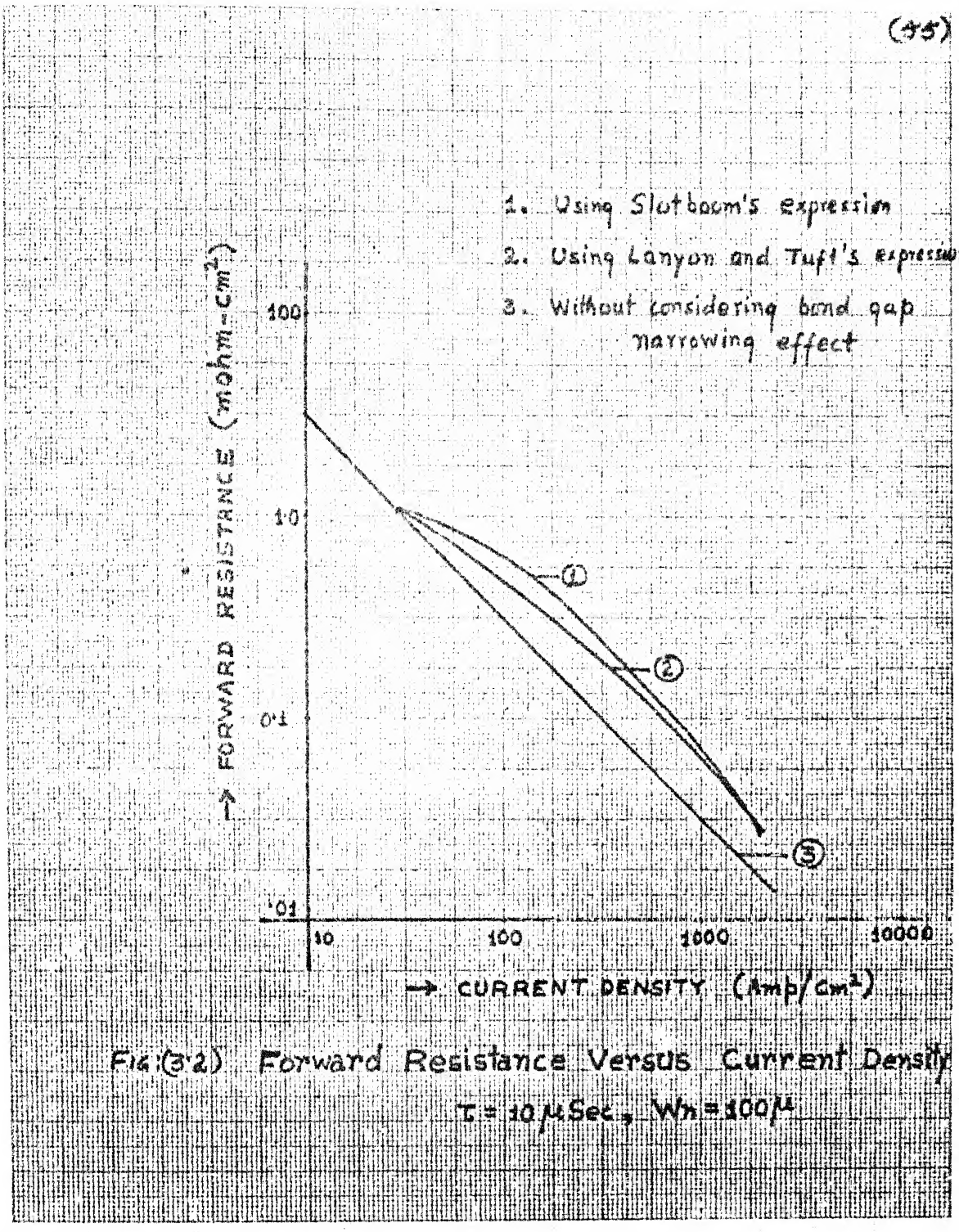

Fig:(3·2) Forward Resistance Versus Current Density

$\tau = 10\,\mu Sec$, $W_n = 100\mu$

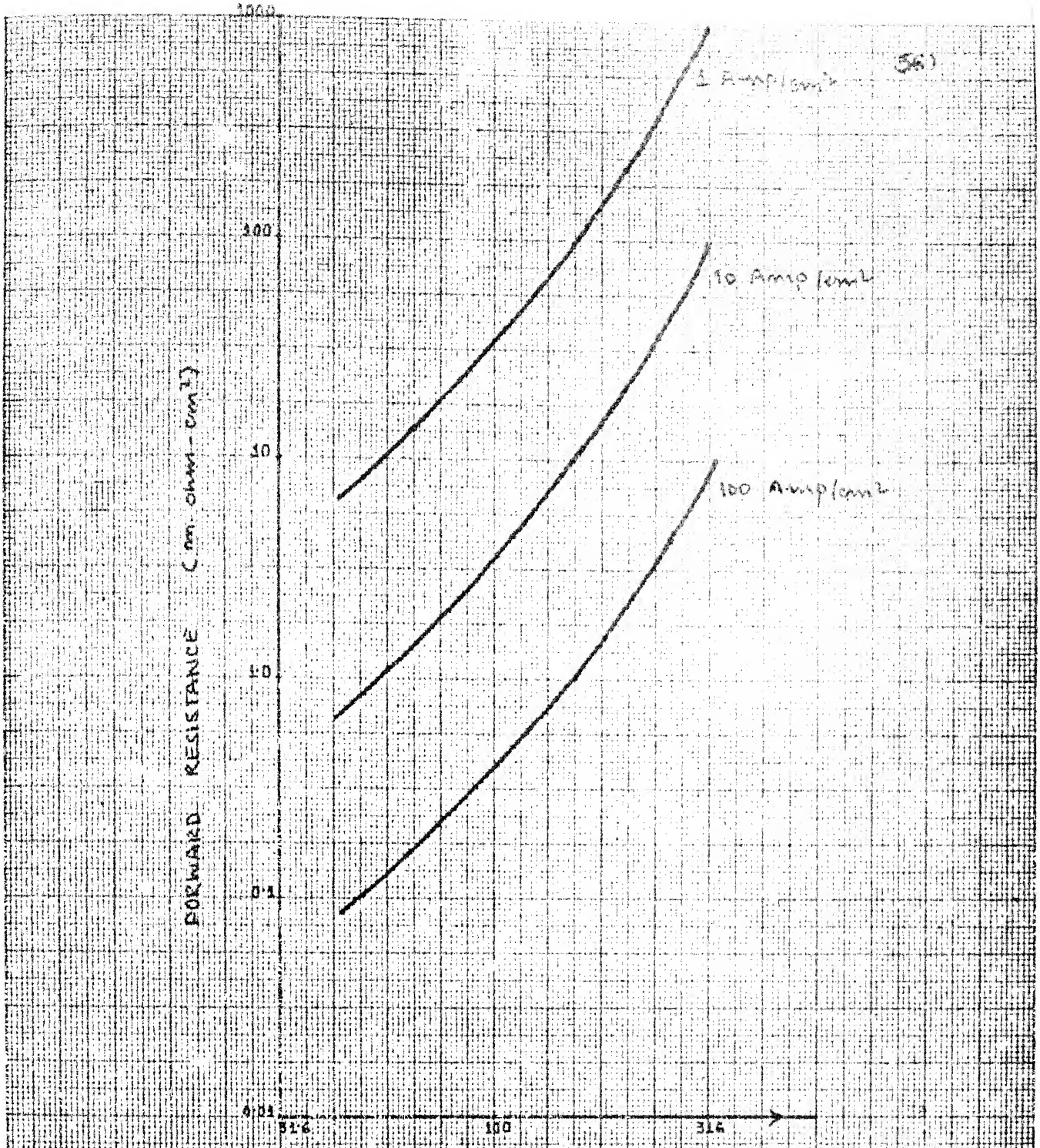

FIG (3.3). Forward resistance versus base region width using Lanyon and Tuft's expression for N_B. $\tau = 1.0$ μsec

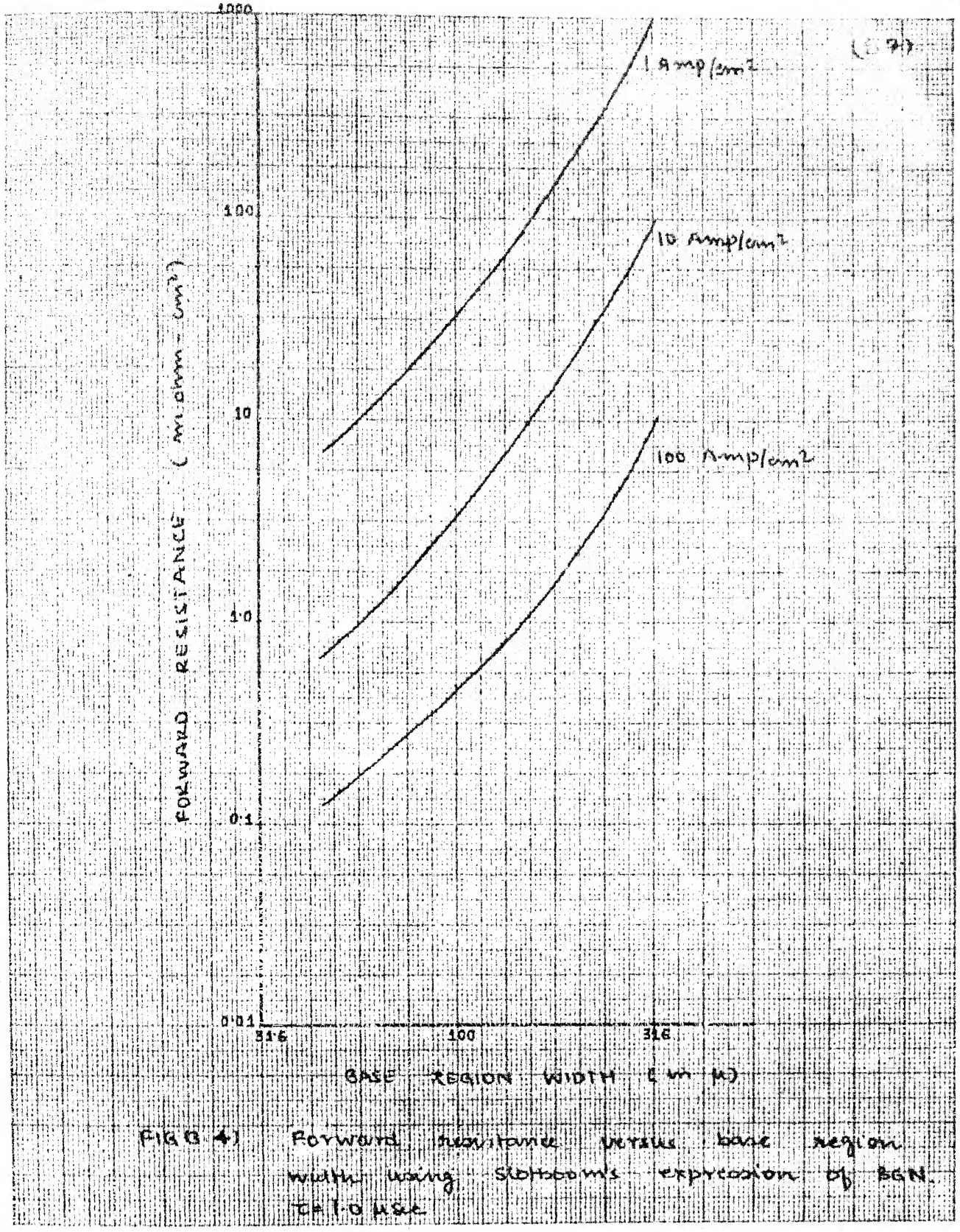

FIG 4) Forward resistance versus base region width using Slotboom's expression of B_{GN}. $\tau_B = 10$ μsec.

Fig 3.1 Forward resistance versus current density using Lanyon and Tuft's expression at 298°K for different T = 10μsec

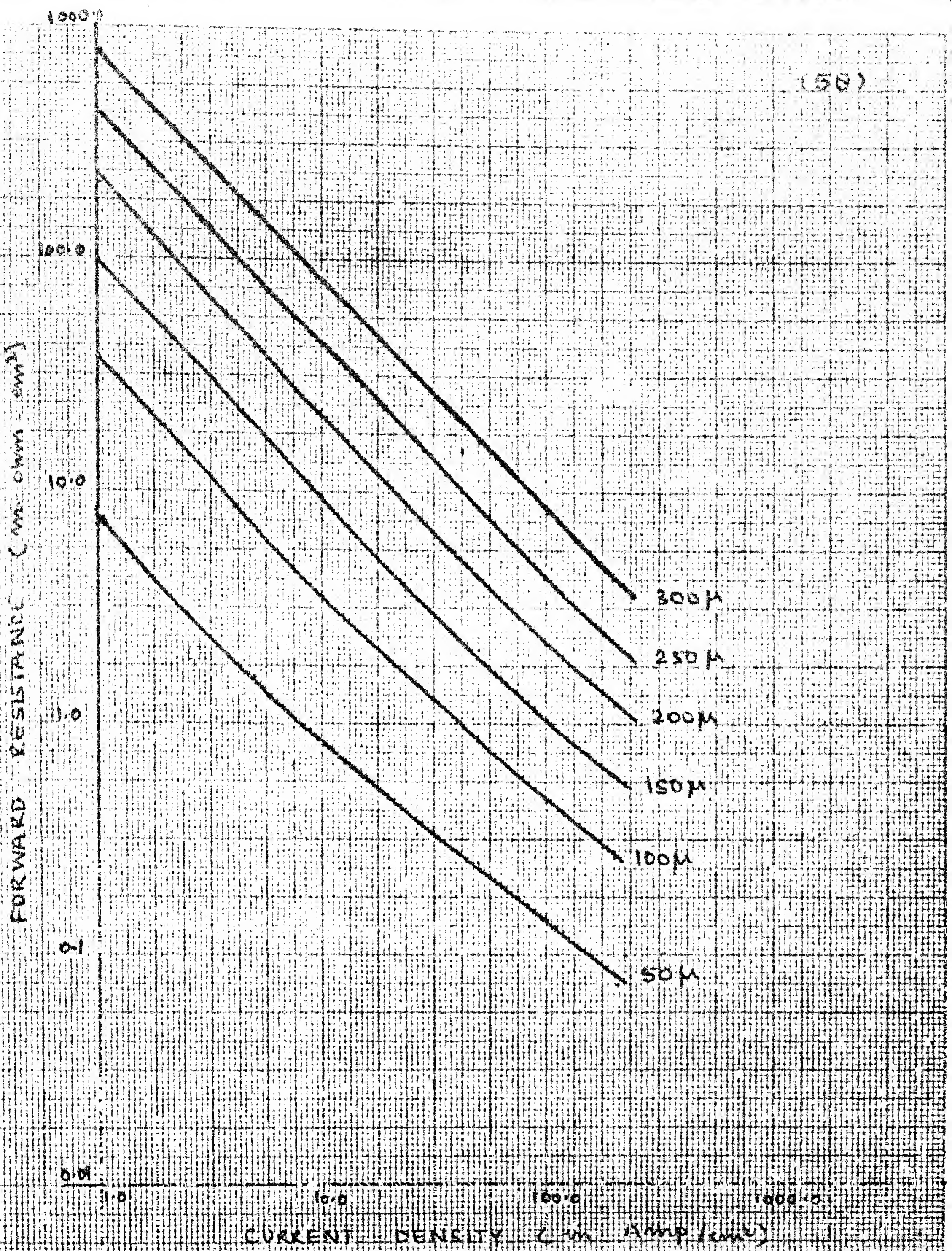

FIG (3.6) Forward resistance versus current density using Strooboom's expression of BGN for different base region width $\tau = 1.0\ \mu sec$

Fig 3.6

that at higher base widths the curve is linear while at lower ones it deviates from linearily at higher currents. The reason being, at base widths of the order of diffusion lengths, the carriers do not recombine. Hence, the band gap narrowing increases which is responsible for the deviation at low base widths.

3.2.2 Life time effects

The effect of life time on forward resistance is an important aspect in the designing of PIN diodes, because it is the life time which degrades during the processing of wafer. Almost every chemical impurity outside of columns III & V of the periodic table exhibits one or more deep impurity levels in Silicon [19] . The amount of these impurities that is incorporated into the silicon depends upon the time and temperature involved. Thus contamination problems are more severe with deep diffused, high voltage structure, PIN diode being one of them. It is observed here, that if one tries to achieve higher breakdown voltage, the forward resistance increases. Attempt was made in our lab to fabricate PIN diodes of breakdown voltage higher than 1000 volts and at the same time the forward resistance should be $\leq$ 0.25 ohms [20] . However, this was not achieved because special care had to be taken to preserve high lifetime during the fabrication. The most important technique to preserve high life time is sealed tube diffusion instead of open tube.

In sealed tube, diffusions are conducted in an oxygen free atmosphere. Silicon dioxide clusters, which are highly mobile at diffusion temperatures, migrate to the surface of the silicon. It is felt that the migration of the oxygen to the surface provides the driving force for the movement of fast diffusing impurities away from the junction region. Thus high life time is preserved. The contamination problem is severe with open tube diffusion, though its effect can be reduced later to some extent by gettering. Halogenic compounds like $POCl_3$, PBr_s & BBr_3 while used as dopants liberate halogenswhich reactswith any impurity in the gas stream as well as with impurities within the silicon that reach to the surface during the diffusion. The reaction converts the impurities into more volatile halides, which leave the system with gas. For metallic gettering, metals such as Nickel or Zinc are first evaporated, on the silicon, which is then heated in an inert atmosphere. Impurities try to move in the layer because of the higher solubility, resulting in an improvement in the life time. Layers of Borosilicate glass (BSG) and Phosphosilicate glass (PSG) are also used for gettering. In fact, this creates diffusion induced defect well ahead of diffusing front. These defects act as a sink for impurities. Thus part of the impurities are removed by out diffusion and rest, piles up in the damaged region under the glass.

To find out the effect of life time, forward resistance is plotted against life time in Fig. 3.7., using Lanyon and

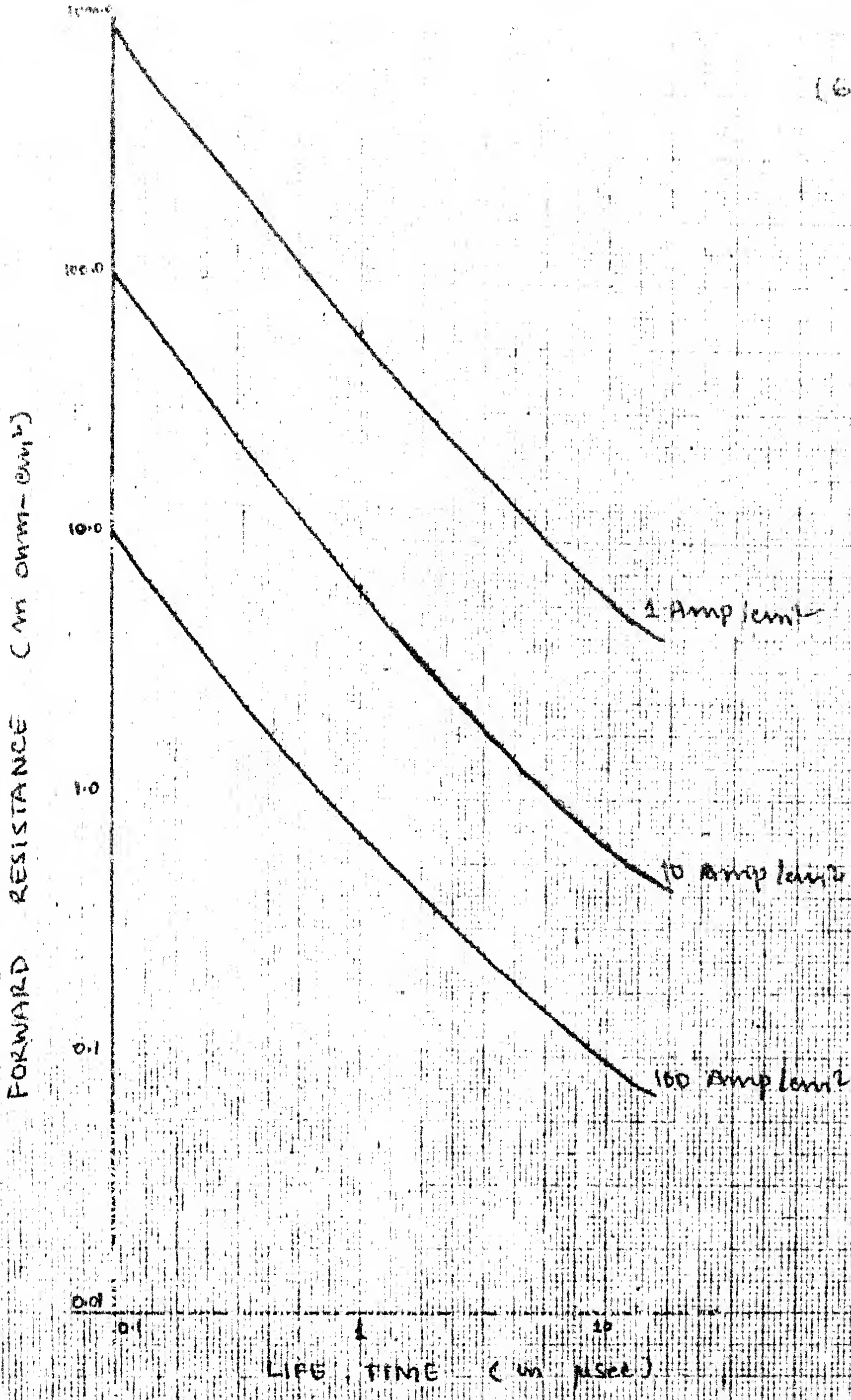

Fig 3.7. Forward resistance versus life time using Lanyon and Tuft's expression of BGN. Wn=100μ.

Tuft's expression for band gap narrowing and Fig. 3.8 using Slotboom's expression. Further, forward resistance is plotted against current density in Figures 3.9 and 3.10. The plot shows that forward resistance increases monotonically with the decrease in lifetime. Quantitatively, if we assume diode area to be 0.0225 cm^2, then for the same current i.e., 22.5 mA, the forward resistance increases from 4.4 Ohms to 42.4 Ohms as the lifetime decreases from 10 μsec to 1 μsec. The reason being that as the lifetime decreases, the recombination rate is increased. Therefore, the charge carriers in the base region decreases and hence the forward resistance increases.

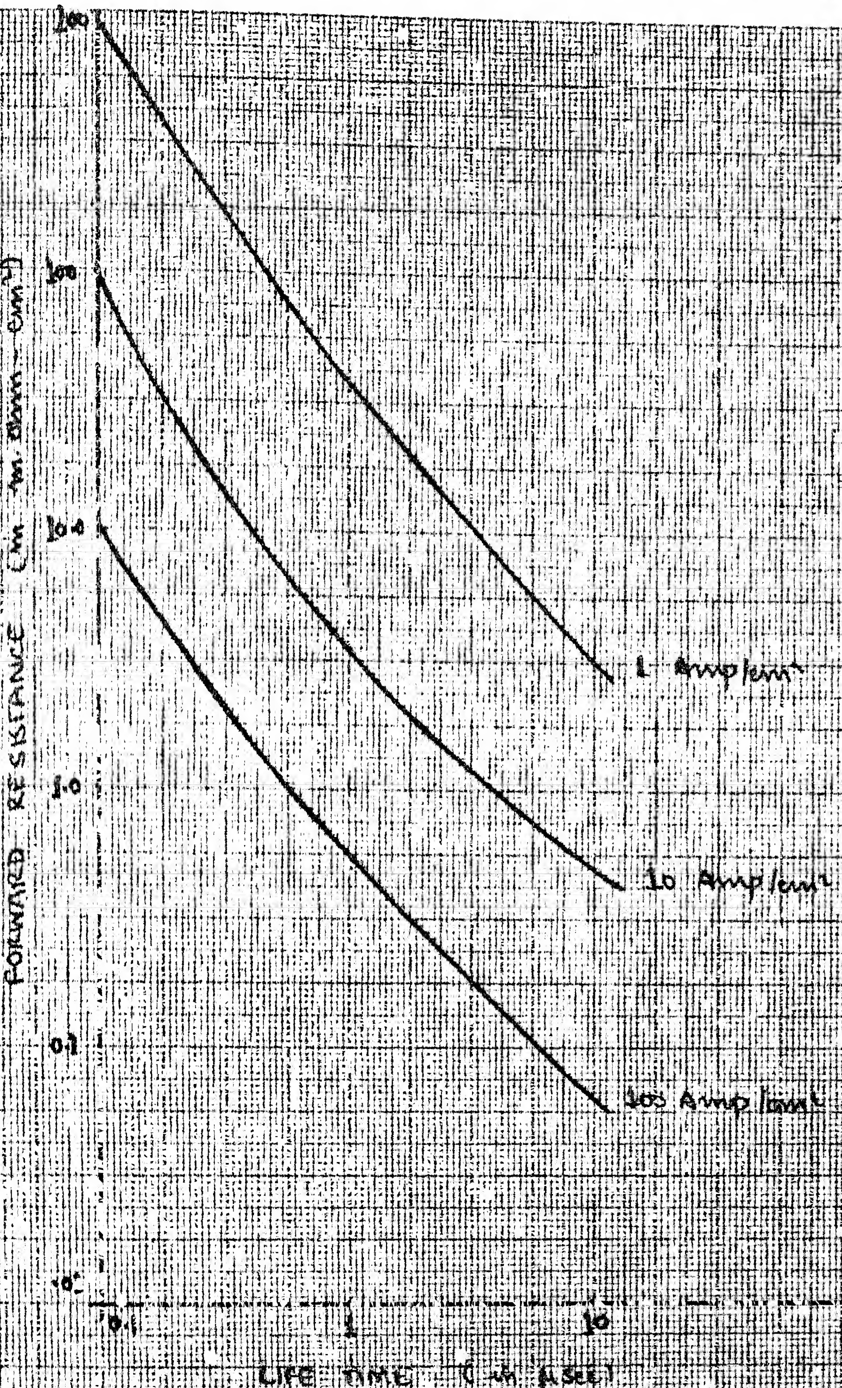

FIG 3.8 FORWARD resistance versus life time using Sutbourn's expression of BCN. Wn = 100 μ

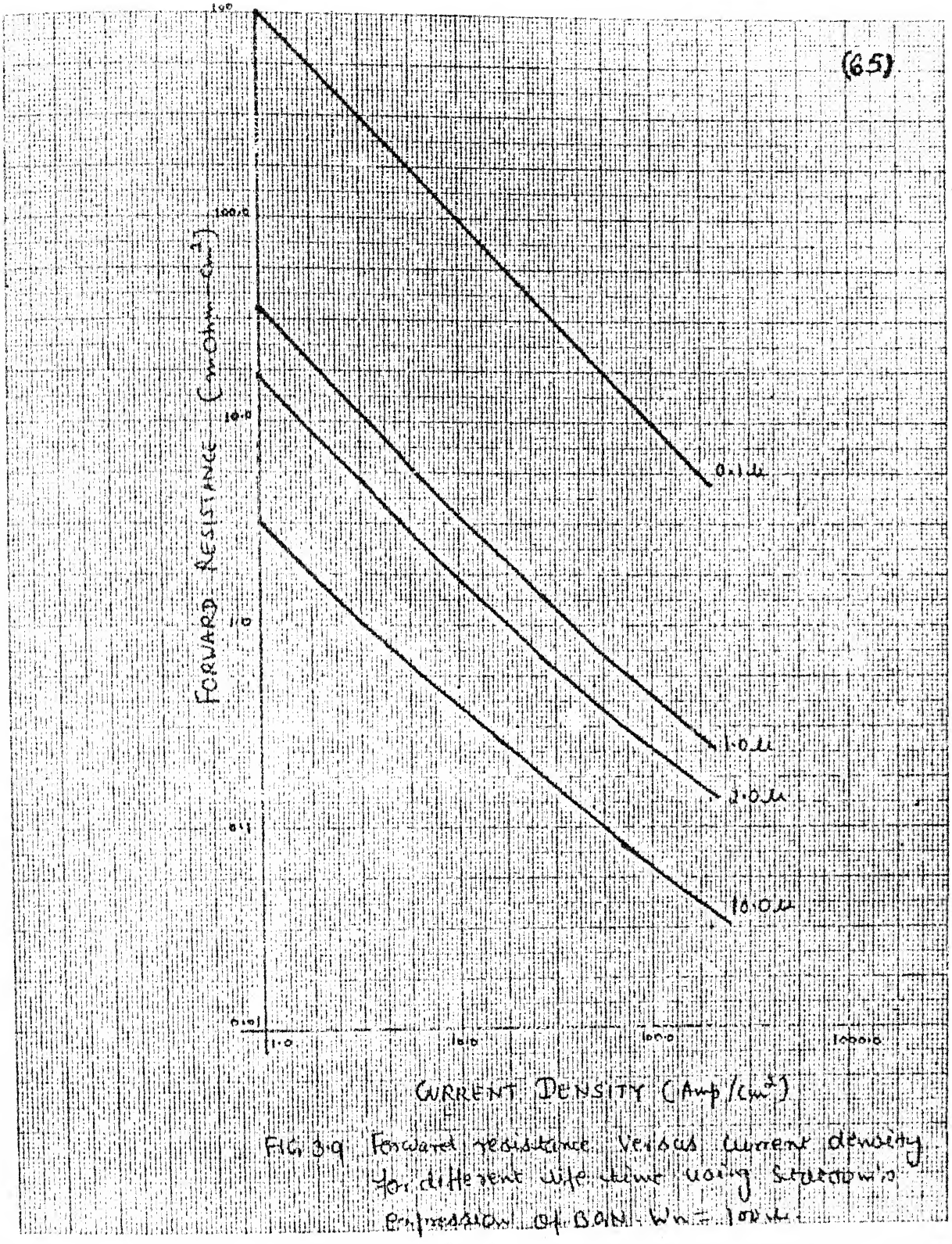

Fig 3.9 Forward resistance Versus current density for different wafer thickness using Shockley's expression of BAM. $W_n = 10\,\mu$

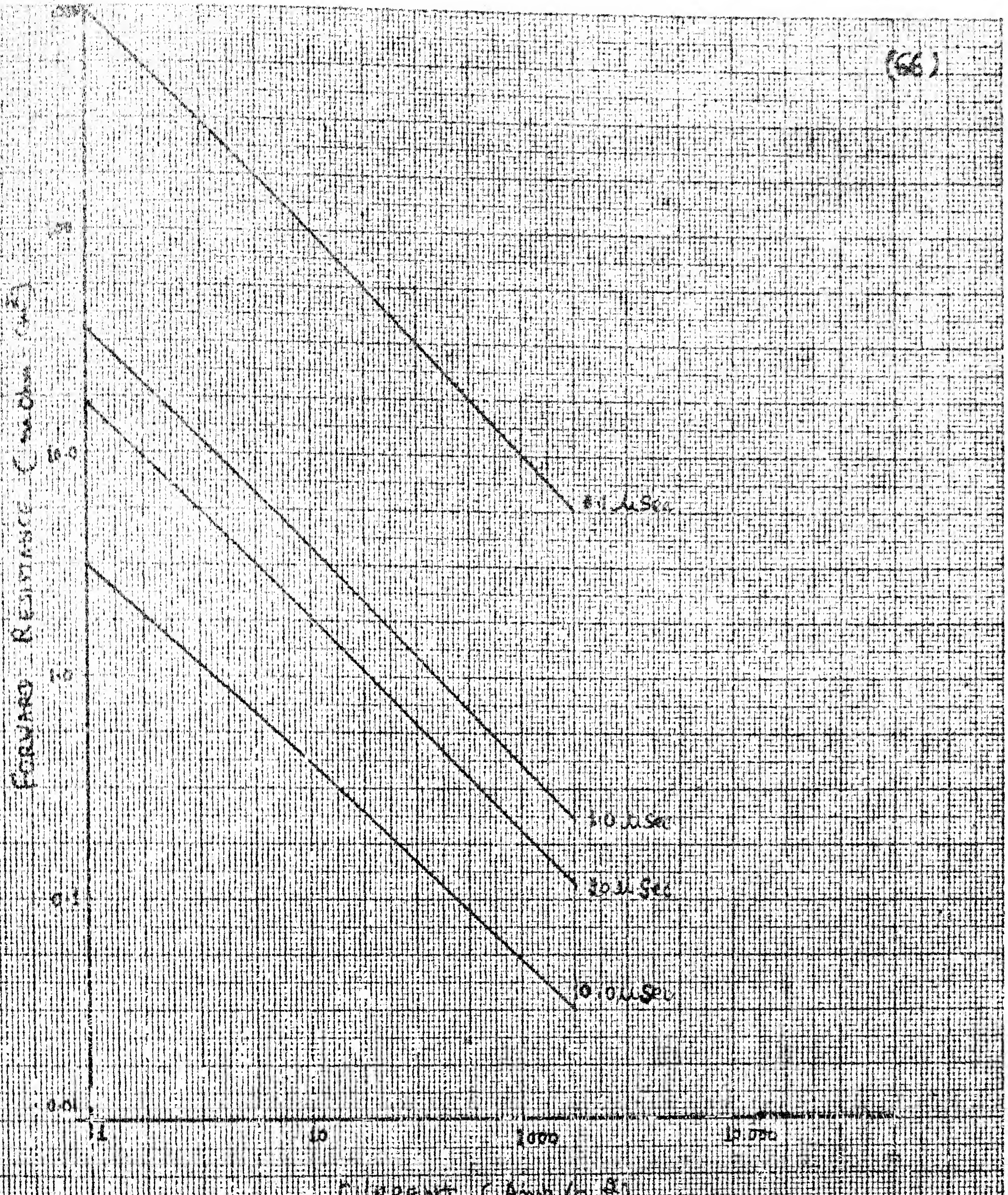

FIG 3.10 Forward resistance versus current for different life time using Lawson and Tufe's expression W=100µ

CHAPTER 4

THE BREAKDOWN VOLTAGE OF PIN DIODE

The breakdown voltage is the most important parameter in the reverse I-V characteristics of PIN diode. The breakdown voltage determines the blocking capability of PIN diode. High voltage PIN diode requires large base widths. But when the base width becomes very much larger than the diffusion length in the base region, the device may no longer be operated efficiently in forward mode. In Section 1.2.2 it is mentioned that there remains always a large difference between the breakdown voltage calculated theoretically using simple models and observed in the fabricated diodes. There are many reasons responsible for this. The first section of this chapter deals with the calculation of breakdown voltage using simple model. Then, some of the reasons responsible for reducing breakdown voltage are discussed, followed by some of the geometries to contour the PIN diode such that its breakdown voltage is increased.

4.1 EFFECT OF HEAVILY DOPED REGION IMPURITY PROFILE

The breakdown voltage is first calculated by taking simple model of constant doping profile in heavily doped regions. But this is very far from the actual profile. Because for high voltage device, deep diffusion is required. Diffusions are performed in two steps, namely the predeposition and drive in

diffusion. In predeposition, the source is present all the time and this results in complementary error function doping profile. In drive in diffusion, which follows the predeposition the source is not present. The impurities already deposited during predeposition are driven in. It results in Gaussian doping profile. Though the complementary error doping profile is closer to the constant doping profile, yet only predeposition can not be used for deep diffusions because of its temperature restrictions. Thus, Gaussian or exponential doping profiles are closest to the profiles in real life diode. Therefore, later, the breakdown voltage is calculated for exponential and Gaussian doping profiles also.

The breakdown voltage essentially depends upon the critical electric field which initiates the avalanching process. The critical electric field is related with the doping level and the ionization integral. At critical electric field, the velocity of the carriers exceed their thermal velocity. When these 'hot' carriers collide with atoms, they impart enough energy to valance band electrons so that they jump in conduction band resulting in the production of hole-electron pair. It starts avalanche process and results in the breakdown. The condition of starting of the avalanche process is that ionization integral should become unity in the depletion region. Thus, in case of P^+ N N^+ structure shown in Fig. 2.2, the condition of breakdown is

$$I = \int_0^{W_n} \alpha_p \exp \{ \int_0^x (\alpha_n - \alpha_p)\, dx' \}\, dx = 1 \qquad (4.1)$$

Where α_n and α_p are the electron and hole ionization coefficients respectively. For silicon ionization coefficient can be written as

$$\alpha(E) = A \exp (-B / |E|) \quad cm^{-1} \qquad (4.2)$$

Where A and B are constants and E is the electric field. The values of A and B are given by [15].

For electrons :

$A = 7.03 \times 10^5$ /cm

$B = 1.231 \times 10^4$ V/cm

for $1.75 \times 10^5 < E < 6.0 \times 10^5$ V/cm

For holes :

$A = 1.582 \times 10^6$ /cm

$B = 2.036 \times 10^6$ V/cm

for $1.75 \times 10^5 < E < 4.0 \times 10^5$ V/cm

and

$A = 6.71 \times 10^5$ /cm

$B = 1.693 \times 10^6$ V/cm

for $4.0 \times 10^5 < E < 6.0 \times 10^5$ V/cm

4.1.1 Constant Doping Profile

For constant doping profile, eqn. (4.1) is solved numerically on computer using Simpson's rule of integration. To find electric field in the base region, Poission's equation in one-dimension has been integrated. Poission's equation for base region is written as

$$\frac{d^2V}{dx^2} - \frac{\rho}{\varepsilon_r \varepsilon_o} = \frac{q N_D}{\varepsilon_r \varepsilon_o} \qquad (4.3)$$

On integrating eqn. (4.3)

$$\frac{dV}{dx} = -E = -\frac{q N_D x}{\varepsilon_r \varepsilon_o} + E_o$$

or

$$E = \frac{q N_D}{\varepsilon_r \varepsilon_o} x - E_o$$

where E_o is the constant of integration and is the electric field at x = 0, i.e., the maximum electric field. It can be written as

$$E_o = \sqrt{\frac{2 q}{\varepsilon_r \varepsilon_o} \cdot N_D} \qquad (4.4)$$

Thus

$$E = \frac{q N_D}{\varepsilon_r \varepsilon_o} x - \sqrt{\left(\frac{2q}{\varepsilon_r \varepsilon_o} N_D\right)} \qquad (4.5)$$

Equation (4.5) shows that electric field is a function of x. During computation, of ionization integral given by eqn. (4.1), electric field is calculated at each point by using eqn.(4.5).

Iterations are made till the value of ionization integral becomes unity. At this point the voltage across PIN diode is breakdown voltage. The breakdown voltage is calculated for different values of doping in the base region and is plotted in Fig. 4.1.

4.1.2 Exponential Doping Profile

The breakdown voltage calculated using constant doping profile is very much larger than the observed values. Therefore, in this section exponential doping profile, which is more realistic than constant doping profile, is assumed. Now the impurity concentration can be written as

$$N(x) = N_{po} \exp\left(-\frac{W_p + X}{L_1}\right) - N_B - N_{no} \exp\left(-\frac{W_{nn} - X}{L_2}\right) \quad (4.6)$$

where N_{po} and N_{no} are the surface concentrations of P^+ and N^+ regions. N_B is the base region impurity concentration L_1, L_2 are constants.

Here also, the electric field can be calculated using Poission's equation. It is written as

$$\frac{d^2V}{dx^2} = -\frac{qN(x)}{\varepsilon_r \varepsilon_o}$$

On integrating

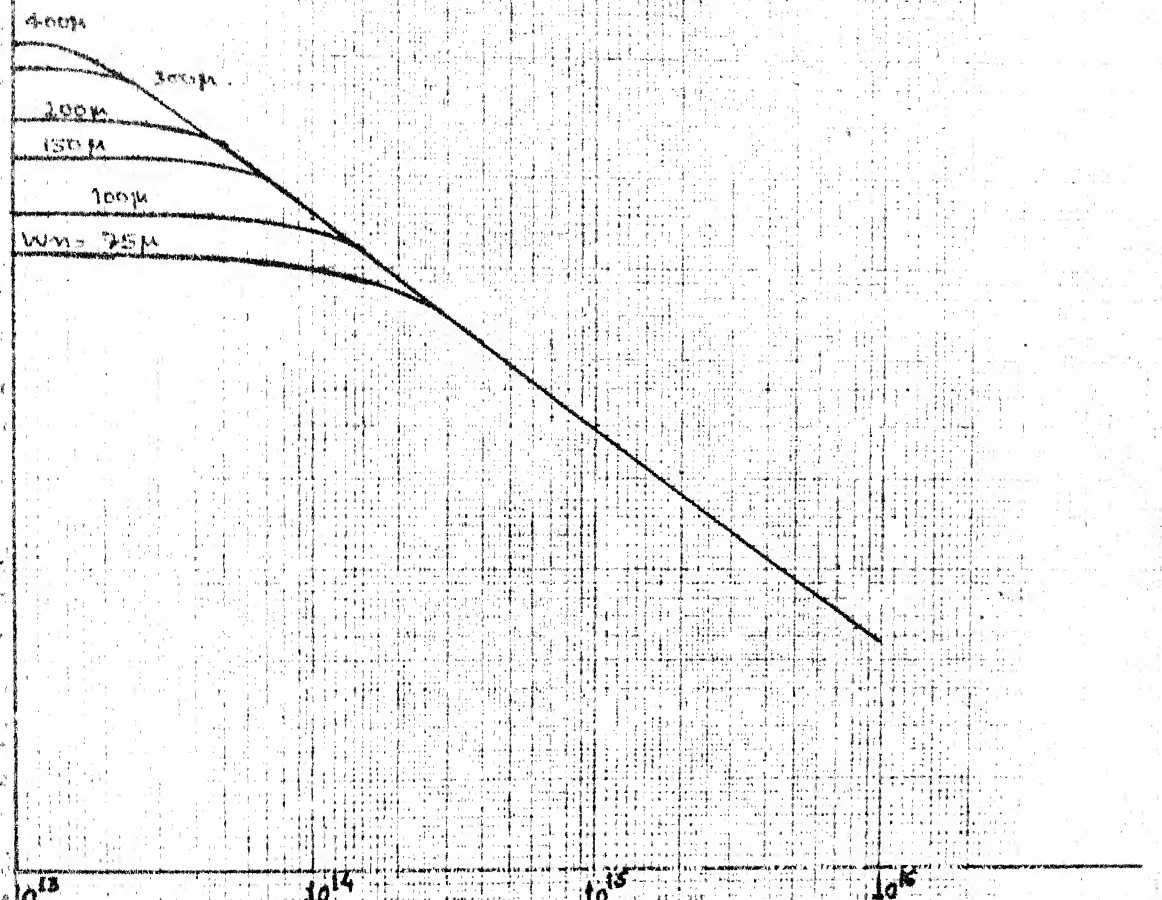

FIG. 4.1 Breakdown voltage as a function of doping concentration for constant doping profile

$$\frac{dV}{dx} = -\frac{q}{\varepsilon_r \varepsilon_o}\int N_{po}\exp\left(-\frac{W_p + X}{L_1}\right) - N_B - N_{NO}\cdot\exp\left(\frac{W_{nn} - x}{L_2}\right) dx$$

$$= -\frac{q}{\varepsilon_r \varepsilon_o}\left[-N_{PO} L_1\cdot\exp\left(-\frac{W_p+x}{L_1}\right) - N_{Bx} - N_{NO} L_2\cdot\exp\left(-\frac{W_{nn} - x}{L_2}\right)\right]$$

$$E(x) = -\frac{dV}{dx}\int_{-p}^{x} = \frac{q}{\varepsilon_r \varepsilon_o}\left[N_{PO} L_1 \exp\left(-\frac{W_p - x_p}{L_1}\right) - N_B x_p\right.$$

$$+ N_{no} L_2 \exp\left(-\frac{W_{nn} + x_1}{L_2}\right) - N_{po} L_1 \exp\left(-\frac{W_p + x}{L_1}\right)$$

$$\left. - N_B x - N_{no} L_2 \exp\left(-\frac{W_{nn} - x}{L_2}\right)\right] \qquad (4.7)$$

Calculating the electric field at every point using (4.7) the ionization integral is solved. Iterations are performed until ionization integral becomes unity. The breakdown voltage is calculated corresponding to that electric field by integrating it. So,

$$V = \int_{-x_p}^{x_n} -\frac{q}{\varepsilon_r \varepsilon_o}\left[N_{po} L_1\cdot\exp\left(-\frac{W_p - x_p}{L_1}\right) - N_B x_p + N_{no} L_2 \exp\left(-\frac{W_{nn} + x_p}{L_2}\right)\right.$$

$$\left. - N_{po} L_1 \exp\left(-\frac{W_p + x}{L_1}\right) - N_B x - N_{no} L_2 \exp\left(-\frac{W_{nn} - x}{L_2}\right)\right] dx$$

or

$$V = -\frac{q}{\varepsilon_r \varepsilon_o}\left[N_{po} L_1 \exp\left(-\frac{W_p - x_p}{L_1}\right).x - N_B x_p x + N_{no} L_2 \exp\left(-\frac{W_{nn} + x_p}{L_2}\right)x\right.$$

$$\left. + N_{po} L_1^2 \exp\left(-\frac{W_p + x}{L_1}\right) - N_B x^2/2 - N_{no} L_2^2 \exp\left(-\frac{W_{nn} - x}{L_2}\right)\right]_{-x_p}^{x_n} \qquad (4.8)$$

The breakdown voltage is calculated for different base region doping concentration and is plotted in Fig. 4.2.

4.1.3 Gaussian Doping Profile

If Gaussian doping profile is assumed, the impurity concentration will be

$$N(x) = N_{po}.\exp(-\frac{W_p+x}{L_1'})^2 - N_B - N_{no}\exp(-\frac{W_{nn}-x}{L_2'})^2 \qquad (4.9)$$

where symbols have same meaning as in eqn. (4.6). L_1' and L_2' are constants.

Since it is difficult to integrate eqn. (4.9) analytically therefore, the electric field at each point is calculated numerically integrating eqn. (4.9). Once again the breakdown voltage is found by iterations as in the previous cases and is plotted in Fig. 4.3.

The breakdown voltage does not differ much when exponential and Gaussian doping profiles are considered. But it reduces appreciably when compared with the values with constant doping profile.

4.2 CAUSES OF PREMATURE BREAKDOWN

If accurate breakdown voltage is to be calculated, then the surface states of the PIN structures must also be considered which are responsible for the reduction in breakdown voltage. This effect is more important in case of plane PIN diodes. Due to contaminated surface and surface state charges, the surface

FIG 4.2 Breakdown voltage as a function of doping concentration in base for exponential doping profile

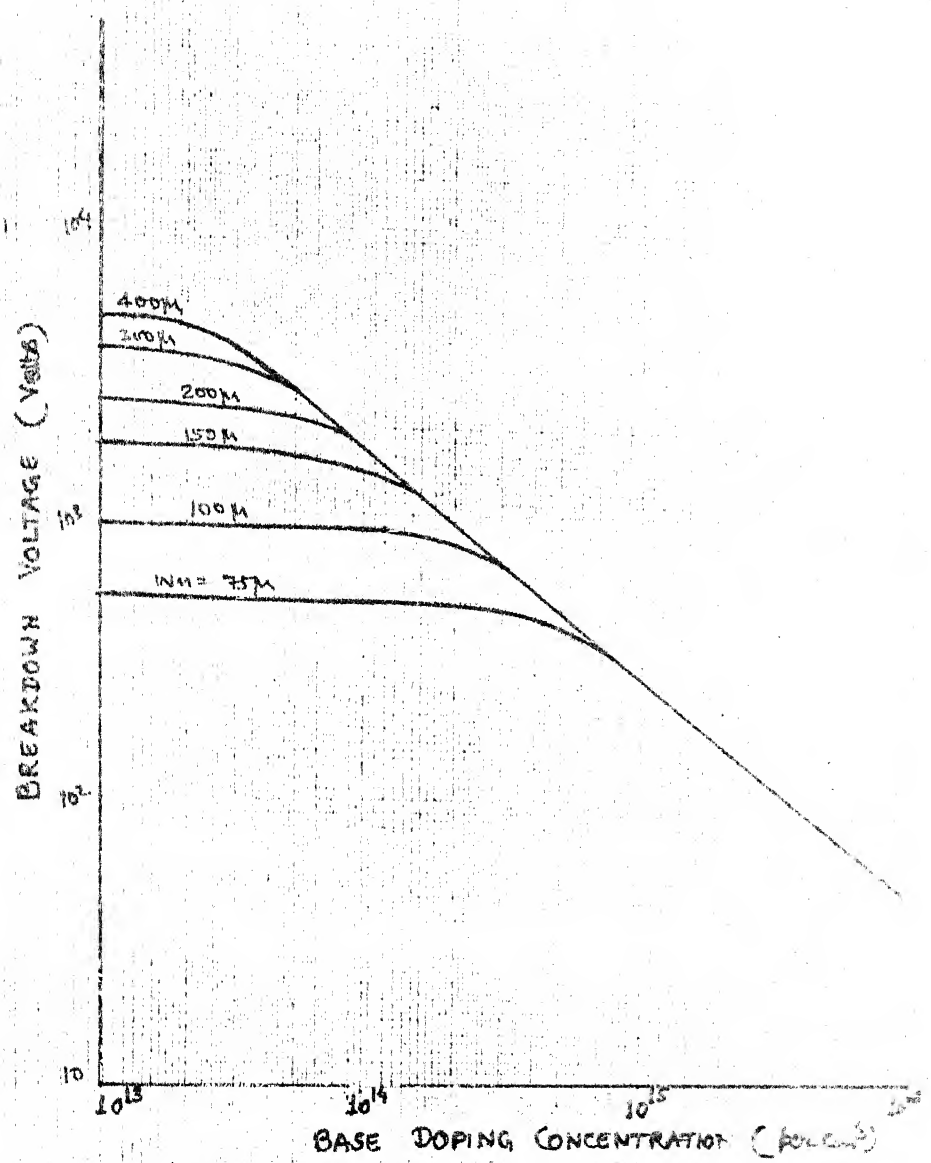

Fig 4.3 Breakdown voltage as a function of doping concentration in base. Gaussian epitaxial profile

electric field changes which may also be the cause of premature breakdown voltage. Calculations which involved surface effects also need a two dimensional analysis. In planar diodes the junction takes a curved surface near the boundary of the semiconductor diffusions, due to lateral diffusion. As a result, the depletion layer in this region is distorted and results in an electric field that differs from parallel plane junction. The calculation shows that electric field is higher at the curvature and this causes the premature breakdown. The problem is more severe with shallow junction. To an approximation, the radius of the cylindrical junction is equal to the junction depth. This can be seen from the figure which shows a n^+P shallow diffused lateral diode. r_1 and r_2 are the radius of the junction and depletion region respectively. On writing Poission's equation in cylindrical form [21].

$$\frac{1}{r}\frac{d}{dr}\left(r\frac{dv}{dr}\right) = -\frac{1}{r}\frac{d}{dr}(rE) = -\frac{q N_A}{\varepsilon_r \varepsilon_o} \qquad (4.10)$$

The boundary conditions are

$$E = E_m \qquad r = r_1$$

$$E = 0 \qquad r = r_2$$

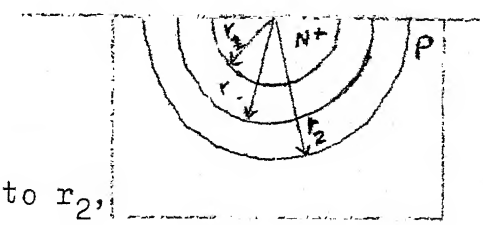

On integrating equation (4.10) from r_1 to r_2,

$$r_1 E_m - 0 = \frac{q N_A}{\varepsilon_r \varepsilon_o}\frac{r^2}{2}\Bigg|_{r_1}^{r_2}$$

or $$E_m = \frac{q N_A}{2\varepsilon_r \varepsilon_o}\frac{r_2^2 - r_1^2}{r_1} \qquad (4.11)$$

Equation (4.11) is further integrated to find out the breakdown voltage. The boundary conditions are

$$V = 0 \qquad r = r_1$$

$$V = -BV \qquad r = r_2$$

The integration gives :

$$BV = \frac{q N_A}{2\varepsilon_r \varepsilon_o} \left(r_2^2 \ln \frac{r_2}{r_1} - \frac{r_2^2 - r_1^2}{2} \right) \tag{4.12}$$

On writing $Y = \frac{2 \varepsilon_r \varepsilon_o}{q N_D r_1}$, and combining eqn. (4.11) and (4.12) to eliminate r_2 results in

$$BV = \frac{\varepsilon_r \varepsilon_o E_m^2}{2q N_A} \frac{2}{Y^2} [(1+Y) \ln(1+Y) - Y] \tag{4.13}$$

The breakdown voltage for parallel plane junction is given by

$$BV_{pp} = \frac{\varepsilon_r \varepsilon_o E_m^2}{2q N_a}$$

Hence

$$\frac{BV}{BV_{pp}} = \frac{2}{Y^2} [(1+Y) \ln(1+Y) - Y] \tag{4.14}$$

BV/BV_{pp} is plotted against Y using equation (4.14) in Figure 4.4. In Y everything else is kept constant excepting r_1. The plot shows that the breakdown voltage of cylindrical junction approaches that of a parallel plane structure for large values of r_1 but falls as the radius is reduced.

Besides this, micro and meso plasmas may also lead to the detoriation of reverse characteristics which are caused by

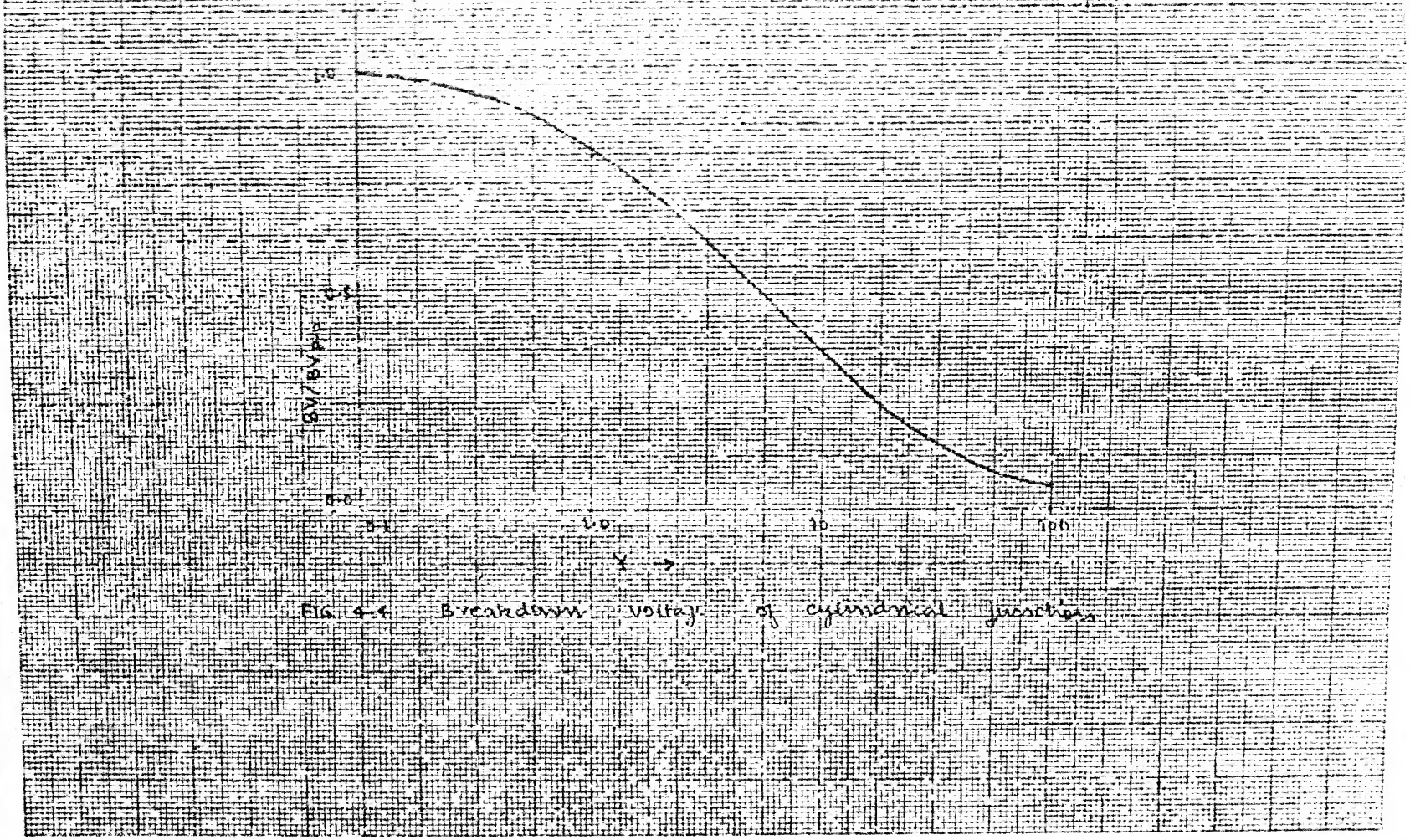

Fig 4.4 Breakdown voltage of cylindrical junction

any inhomogeneity in the crystal. The inhomogeneity can come about as a material property because of structural or doping imperfections. Microplasma consists of quasi neutral regions flooded with holes and electrons in almost equal numbers. It is described by three constants [22] a voltage V_B, a time τ_o and a current I_1. If the voltage is below V_B, the microplasma is off and carries negligible current. If the voltage rises above V_B, the microplasma on an average waits for a time τ_o and then switches on and carries a current I_1. As the voltage drops below V_B, the microplasma at once switch off. Microplasma is inherently stable. In steady state, the rate of electron - hole pair production in a microplasma is equal to the rate of loss of carriers from the filament by diffusion. Thus an increase in the rate of pair production, e.g., by raising the applied voltage, will be balanced by an increase in filament diameter, until a new steady state condition is reached. This is true as long as the local temperature is below the intrinsic temperature, where intrinsic temperature is defined as the temperature at which carrier concentration due to thermal effects becomes equal to the background concentration. Beyond this temperature, the generation of electron hole pairs can advance rapidly and independently of the electric field, accompanied by a rapid local rise in temperature. This is accompanied by a rise in the current density, resulting in the formation of the giant plasma.

The establishment of microplasma results in an irreversible damage to the device. This failure mode is referred to as second breakdown. It is defined to a transition to a state of higher conductance in a reverse biased avalanching semiconductor device. On studying second breakdown [23] by applying short high amplitude current pulses, it was found that these is a delay time between the application of a pulse and onset of second breakdown transition. When the current pulse is applied, the junction temperature reaches to a critical value and the voltage starts falling [24]. However, the junction temperature is never uniform because of the inhomogeneties. Thus at a localised site the voltage will drop faster than in the surrounding regions, which will lead to current channeling. This will increase the temperature further and consequently the channeling will increase. With this the junction ceases to avalanche locally, because the voltage falls at nucleation site. The distribution of current in the neighbourhood of nucleation site is modified and the current funnels into the channel as shown in Fig. 4.5, Accompanying the converging current is the spreading resistance that ballasts the channel and produces a potential gradient along the junction. When the voltage reaches the avalanche voltage V_B, the junction again conducts. The voltage across the device does not change appreciably with the formation of junction channels like this.

The growth of the filament channel increases as the local region reaches the temperature T_2 after which the resistivity starts falling, as shown in the temperature - resistivity

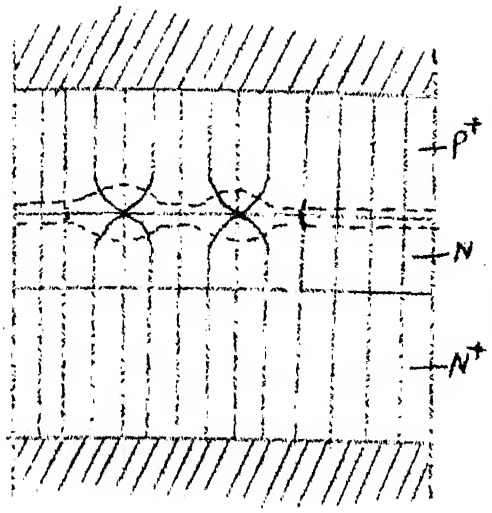

Fig.4.5 Current Distribution in Reverse Biased Diode showing Channeling

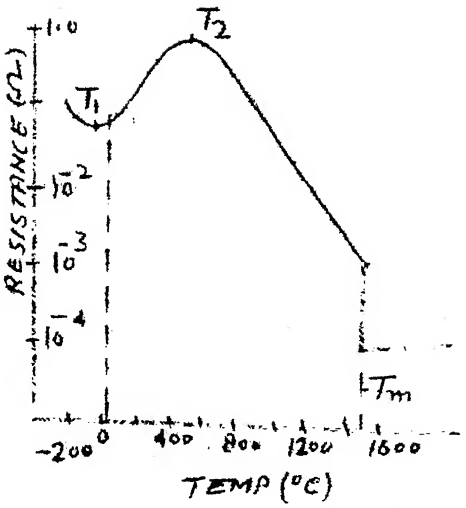

Fig.4.6 Temperature Resistivity Curve for n-type Silicon. T_m is Melting Point

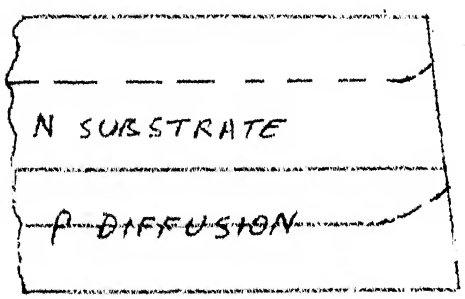

Fig.4.7a Positive Bevelling

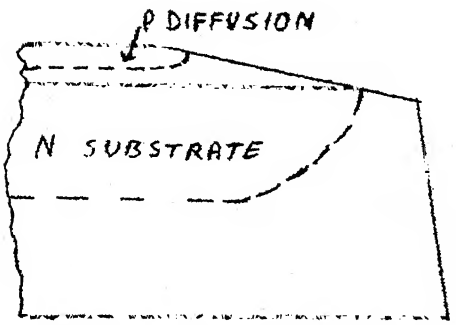

Fig.4.7b Negative Bevelling

curve in Fig. 4.6 [23]. Between temperature T_2 and T_m, an increase in local temperature produces an increase in local current, which tends to increase the temperature further. (The process continues until heat sinking or circuit constraints prevent further temperature rise or the device is destroyed). During the growth the filament is stabilized by series resistance of the portion of the high resistivity region (which is at a temperature less than T_2) that feeds the element. The temperature at the center of the filament rises will above T_2. When the filaments bridges the high resistivity region, the temperature at its center rises still further and a melt is formed, a narrow high conductance region that replaces the original filament. This is the destructive form of second breakdown.

4.3 GEOMETRIES TO IMPROVE BREAKDOWN

However, one can improve the breakdown voltage by surface contouring in case of plane diodes and by providing diffused guard rings or field plate in planar diodes.

4.3.1 In Plane Diodes

The surface contouring geometries include positive bevelling, negative bevelling, deep moat etch, depletion etch method and substrate etch method.

A positive bevelled junction shown in Fig.4.7(a) is one that results in a junction of decreasing area when going from the heavily doped side to the lightly doped side. The positive

bevelling results in a surface electric field that is less than what it would be if the junction had not been bevelled. Also the position of peak surface electric field shifts from the metallurgical junction and into the lightly doped side.

A negative bevelled junction is one that results in a junction of decreasing area when joining from the lightly doped side to the heavily doped side. In this case, the peak electric field may either increase or decrease depending upon the angle and the impurity distribution. Generally, in highly assymetric junctions, the edge of the depletion region on lightly doped side moves much further than that on the heavily doped side. Therefore as the angle is reduced from 90° the field increases until the edge on the lightly doped side reaches the junction. The field is maximum at this angle. Reduction of the surface field occurs with further reduction in angle magnitude because the surface of the depletion region on heavily doped side is increasing.

Both positive and negative bevelling have the drawback that these require mechanical grinding of the surface. Furthermore, processing steps like passivation etc., which follow the bevel step are to be done on individual chips. Therefore some other geometries depending upon the same principle are described which include deep moat etch, depletion etch method and substrate etch geometry which are shown in Fig. 4.8(a), (b) and (c).

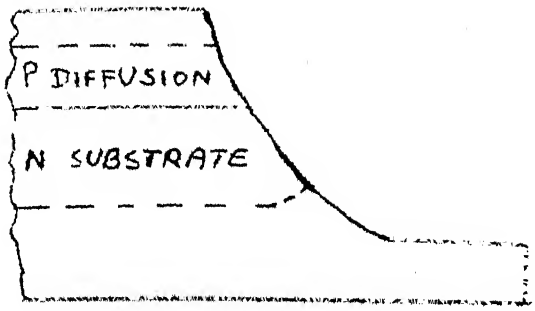

Fig. 4.8a Deep Moat Etch

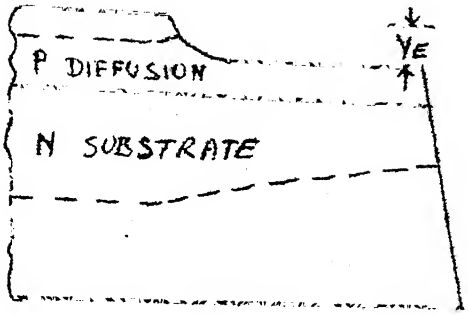

Fig. 4.8b Depletion etch method

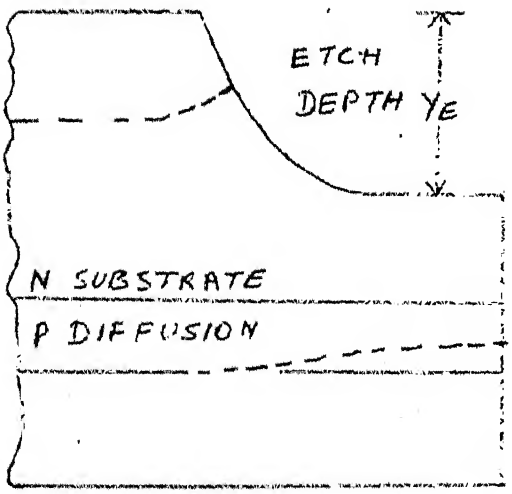

Fig.4.8c Substrate Etch Geometry

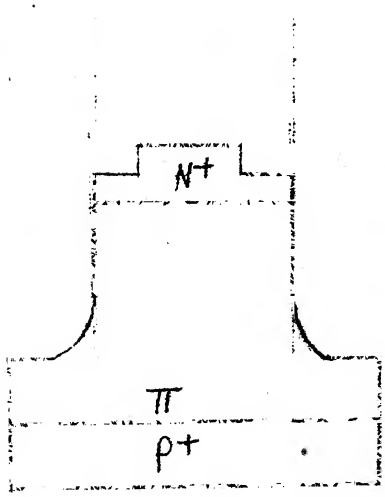

Fig.4.8d Geometry Proposed by Korde & Hasan

The deep moat etch is used where many devices have to be fabricated on single wafer. In this method, the breakdown voltage is generally 60 to 80% of the ideal breakdown voltage and depends upon the effectiveness of the passivation. Adler and Temple [25] observed that very close to ideal breakdown voltage can be achieved in plane diodes using depletion etch method. The results were comparable with those obtained with negative bevel but with the lesser loss of device area. The main problem with this method is that the etch depth is critical and requires micron accuracy. Same authors [26] later described another geometry named substrate etch geometry. The substrate etch geometry bears the same relationship with positive bevelling as the depletion etch method with the negative bevelling. It is observed that etch into the depletion region on the lightly doped side is effective in reducing the peak surface electric field, while not increasing the peak bulk electric field. It is further shown that this geometry results in the enhanced breakdown voltage over a wide range of etch depths.

4.3.2 In Planar Diodes

In planar diodes, the curvature of the depletion layer near the boundaries of diffusion results in the premature breakdown. The curvature can be controlled the same extent by using following geometries [19].

Diffused guard rings could be used to force the curvature of the depletion layer in opposite direction so as to avoid edge breakdown. Fig. 4.9a shows such type of structure in which deep n^+ type annular rings are first diffused, which is followed by a n^+ shallow diffusion. The deep annular diffusion is designed to have a breakdown voltage higher than the breakdown voltage of the shallow diffusions in parallel plane regions.

The other method to control the depletion layer curvature near the edge of the diffusion is to provide field plates. It is particularly suitable for diffused junctions made by photo-masked processes. A n^+P diode having field plate is shown in the Fig. 4.9b. If a positive voltage will be applied, it will increase the curvature by making the underlying semiconductor more P type. While a negative voltage at field plate will make the underlying semiconductor less P type and hence the depletion layer curvature will be reduced. Thus the depletion layer curvature can be controlled by the polarity and magnitude of the voltage applied at the field plate.

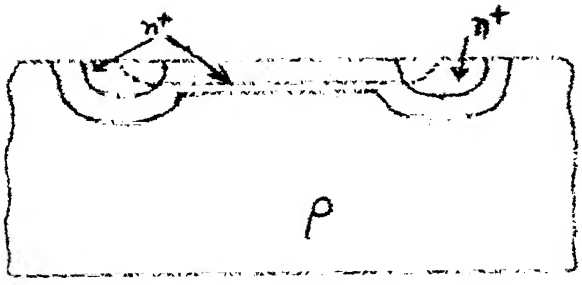

Fig. 4.9a Diffused guard ring structure

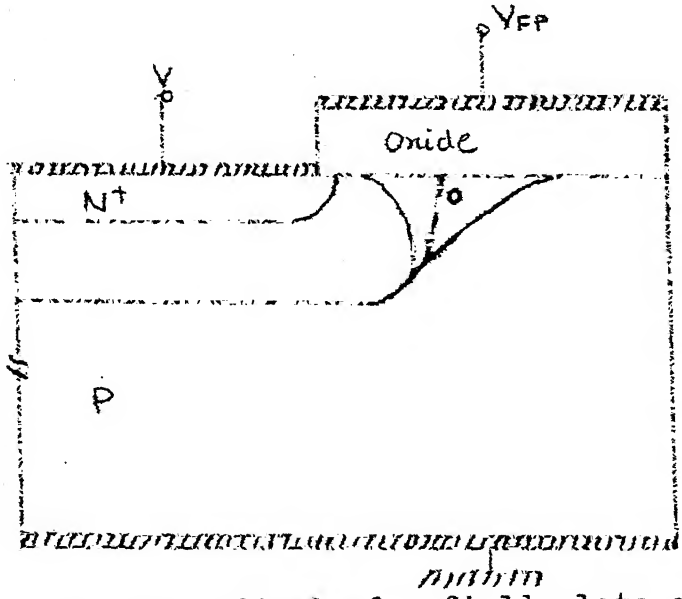

Fig. 4.9b The effect of a field plate on the depletion layer

Hence, for accurate prediction of breakdown voltage one has to take into consideration all the effects discussed earlier and to bring the breakdown voltage closer to the theoretical limit proper contouring of the surface is normally done. These techniques are used in the case of high voltage rectifier diode as well as SCR.

CHAPTER 5

CONCLUSION

The forward I-V characteristics of the PIN diode is calculated. It is seen that band gap narrowing, the result of heavy doping, does influence the I-V characteristics. At low currents, the band gap narrowing does not alter the I-V characteristics. But if the life time is very much increased, the forward characteristics at low currents is also influenced. At high currents, the band gap narrowing effects the forward characteristics. At low currents the forward voltage decreases with the increase in life-time upto a certain value of lifetime, after which it again starts increasing. At high currents, initially the forward voltage decreases, but later it becomes constant. Thus, there is an optimum lifetime for which the voltage drop is minimum. It also points out that the control of lifetime is important in the fabrication of PIN diode.

The forward resistance increases if the band gap narrowing effect is considered. The increase is dependent on base region width as well as lifetime. The increase is more for diodes having large base region width and high carrier lifetime.

In the reverse characteristics the breakdown voltage is studied. It is found that the breakdown voltage is dependent on the impurity gradients at the junctions. The contaminated

surface and curvature of depletion region are the main factors due to which electric field is increased at a particular ~~reason~~ region only and pre-mature breakdown occurs. Besides this, meso-plasma also results in the reduction of breakdown voltage. The proper contouring of the surface, diffused guard ring and field plates help in avoiding pre-mature breakdown.

REFERENCES

1. Prince, M.B., 'Diffused p-n junction Silicon Rectifiers', Bell Syst. Tech. J., 35, pp. 661-684 (May, 1956).

2. Uhlir, A. Jr., 'The Potentials of Semiconductor Diodes in High Frequency Communication', Proc. IRE 46, pp.1099-1115 (June, 1958).

3. Hall, R.N., 'Power Rectifiers and Transistors', Proc. IRE, 40, pp. 1512-1518, (November, 1952).

4. Kleinman, D.A., 'The Forward Characteristic of the PIN Diode', Bell Syst. Tech. J. 35, pp. 685-706, (May, 1956).

5. Fletcher, H.H., 'The High Current Limit for Semiconductor Junction Devices', Proc. IRE, 45, pp. 862-872, (June, 1957).

6. Howard, N.R. and Johnson, G.W., 'PIN Silicon Diodes at High Forward Current Densities', Solid State Electron., 8, pp. 275-284 (1965).

7. Herlet, A., 'The Forward Characteristic of Silicon Power Rectifiers at High Current Densities', Solid State Electron., No.8, pp. 717-742 (1968).

8. Choo, S.C., 'Effect of Carrier Lifetime on the Forward Characteristics of High Power Devices', IEEE Trans. on Electron Devices, ED-17, pp. 647-652 (September, 1970).

9. Kao, Y.C. and Muss, D.R., 'Analytical Design Theory for High Voltage PIN Rectifiers', Solid State Electronics, 13, pp. 825-841 (June, 1970).

10. Graham, E.D. Jr. and Hauser, J.R., 'Effects of Base Doping and Width on the J-V Characteristics of the n^+-n-p^+ Structure', Solid State Electronics, 15, 303-310 (March,1972).

11. Kauffman, W.L. and Bergh, A.A., 'The Temperature Difference of Ideal Gain in Double Diffused Silicon Transistors', IEEE Trans. on Electron Devices, ED-15, pp. 732-735 (1968).

12. Buhanan, D., 'Investigation of Current Gain Temperature Dependence in Silicon Transistors', IEEE Trans. on Electron Device, ED-16, pp. 117-124 (January, 1969).

13. DeMan, H.J.J., 'The Influence of Heavy Doping on the Emitter Efficiency of a Bipolar Transistor', IEEE Trans. on Electron Device, ED-18, pp. 833-835 (October, 1971).

14. Van Overstraeten, R.J., DeMan, H.J.J. and Mertens, R.P., 'Transport Equations in Heavy Doped Silicon', IEEE Trans. on Electron Device, ED-20, pp. 290-298 (March, 1973).

15. Lanyon, H.P.D. and Tuft,R.A., 'Bandgap Narrowing in Moderately to Heavily Doped Silicon', IEEE Trans. on Electron Device, ED-26, pp. 1014-1015 (July, 1979).

16. Vol'fson, A.A. and Subashiev,V.K., 'Fundamental Absorption Edge of Silicon Heavily Doped with Donor or Acceptor Impurities', Sov. Phys. - Semicond., 1, pp. 327-332, (September 1967).

17. Van Overstraeten, R.J., 'Measurements of the Ionization Rates in Diffused Silicon p-n Junction', Solid State Electron. 13, pp. 583-607 (1970).

18. Slotboom, J.W. and De Graff, H.C., 'Measurements of Band Gap Narrowing in Silicon Bipolar Transistors', Solid State Electron. 19, pp. 857-862 (1976).

19. Ghandhi, S.K., 'Semiconductor Power Devices', John Wiley & Sons, New York (1977).

20. Ghandhi, S.K., 'The Theory and Practice of Microelectronics', John Wiley & Sons, New York (1968).

21. Korde, R.S., 'Studies on the Process Control of Device Parameters of Silicon PIN Diodes', Ph.D. Thesis, I.I.T. Kanpur (October, 1979).

22. Haitz, R.H., Goetzberger, A., Scarlett, R.M. and Shockley,W., 'Avalanche Effects in Silicon p-n Junctions - Part I', J. of Applied Physics, 34, pp. 1581-1590 (June, 1963).

23. Smith, W.B., Poutius, D.H. and Budenstein, P.P., 'Second Breakdown and Damages in Junction Devices', IEEE Trans. on Electron Device, ED-20, pp. 731- , (August, 1973).

24. Weitzsch, F., 'A Discussion of Some Known Physical Models for Second Breakdown', IEEE Trans. on Electron Device, ED-13, pp. 731-734 (November, 1966).

25. Temple, V.A.K. and Adler, M.S., 'The Theory and Application of a Simple Etch Contour for Near-Ideal Breakdown Voltage in Plane and Planar P-N Junctions', IEEE Trans. on Electron Device, ED-23, pp. 950-955 (1976).

26. Temple, V.A.K. and Adler, M.S., 'A Substrate Etch Geometry for Near Ideal Breakdown Voltage in p-n Junction Devices', IEEE Trans. on Electron Device, ED-24, pp.1077-1081, (August, 1977).

27. Korde, R.S., Khurana, K.K. and Hasan, M.M., 'Enhancement of the Breakdown Voltage of PIN Diode by Etch Contour', Proc. Symposium on Electron Devices CEERI, Pilani, pp. 5.23-5.28 (September, 1978).

28. Milnes, A.G., 'Deep Impurities in Semiconductors', John Wiley & Sons, New York (1973).